www.sciencemag.org/content/346/6211/861/suppl/DC1

Supplementary Material for

Prevention and cure of rotavirus infection via TLR5/NLRC4–mediated production of IL-22 and IL-18

Benyue Zhang, Benoit Chassaing, Zhenda Shi, Robin Uchiyama, Zhan Zhang, Timothy L. Denning, Sue E. Crawford, Andrea J. Pruijssers, Jason A. Iskarpatyoti, Mary K. Estes, Terence S. Dermody, Wenjun Ouyang, Ifor R. Williams, Matam Vijay-Kumar, Andrew T. Gewirtz*

*Corresponding Author. E-mail: agewirtz@gsu.edu

Published 14 November 2014, *Science* **346**, 861 (2014)
DOI: 10.1126/science.1256999

This PDF file includes:

Materials and Methods

Figs. S1 to S22

Full Reference List

Materials and Methods

Mice. WT C57BL/6, *Rag1*$^{-/-}$, *IFNγR1*$^{-/-}$, *Il1r*$^{-/-}$, *Il18*$^{-/-}$, *p40*$^{-/-}$, CD11c -DTR, *Rag2/Il2rg*$^{-/-}$ and CD45.1 transgenic mice (on C57BL/6 background) were obtained from Jackson Laboratories (Bar Harbor, ME). IFN I & II R$^{-/-}$ and *STAT1*$^{-/-}$ mice, on a C57BL/6 background, were gifts from Dr. Herbert Virgin (Washington University, St. Louis, MO). *IFN I R*$^{-/-}$ mice, which were on a 129 S2 background, were a gift of Dr. Sam Speck (Emory University, Atlanta, GA). *Nlrc4*$^{-/-}$ and *Il22*$^{-/-}$ mice were provided by Genentech, Inc (South San Francisco, CA). *Tlr5*$^{-/-}$ and *MyD88*$^{-/-}$ mice were originally generated by Dr. Shizuo Akira (Osaka University, Japan) and backcrossed to C57BL/6 mice for 10 generations. Generation of *Tlr5/Nlrc4*$^{-/-}$ was previously described (*14*). Human IL-18 binding protein (BP) transgenic mice were generated by Dr. Charles Dinarello (University of Colorado, Denver, CO) and maintained as previously described (*12*).

Materials. FliC isoform of flagellin was HPLC-purified, and purity was verified as previously described (*26-29*). Briefly, flagella were isolated from FljB-deficient *S. typhimurium* strain *SL3201fljB*$^{-}$ via high-speed centrifugation of bacterial supernatant. Flagella were converted to flagellin monomers by boiling. Flagellin monomers were chromatographically purified using polymixin B agarose, S-sepharose, and Q-separose. This procedure results in a preparation of flagellin that does not activate gene expression (as assessed by RT-PCR and microarray) in mice lacking both known flagellin receptors indicating it does not contain levels of innate immune agonists beyond flagellin. Murine IL-22 was provided Genentech, Inc. Murine IL-18 was purchased from Sino Biologicals Inc. (Beijing, China). Human IL-22 was purchased from BioLegend (Sand Diego CA). Human IL-18 was purchased from Invivogen (San Diego, CA). Flt3 ligand was a gift of Dr. Robert Mittler (Emory University, Atlanta, GA).

Rotavirus infection and flagellin and cytokines treatment. *Acute models*- Mice were infected with a range of dilutions of a preparation of murine rotavirus EC strain by oral inoculation to determine the amount of virus that resulted in 50% of mice exhibiting a course of detectable fecal RV antigens, referred to as SD50 as per previous studies. Mice were infected with 10^5 SD50 of murine rotavirus EC strain by oral inoculation after feeding 100 µl of 1.33% sodium bicarbonate to neutralize stomach acid. Except for diarrhea studies and chronic infection studies, we utilized 8-12-week-old mice and gavage volume of 100 µl. Flagellin treatment, unless indicated otherwise, used a dose of 20 µg in 0.2 ml PBS, or 0.2 ml PBS as control, which was given 2 hours prior to inoculation and on days 2, 4, 6 and 8 p.i. *Diarrhea model*- 7-day-old mice were inoculated with 400 SD50 administered in 50 µl PBS. Flagellin treatment, unless indicated otherwise, used a dose of 10 µg and was given 2 hours prior to inoculation and daily on days 0-9 p.i. *Chronic model*- Chronic rotavirus infection was performed as previous described (*9*). Briefly, 3-week-old *Rag1*$^{-/-}$ mice were fed with 100 µl of 1.33% sodium bicarbonate and then infected with 10^5 SD50 of murine rotavirus EC strain by oral inoculation. Feces were collected at 3 weeks after infection to confirm the establishment of chronic infection. Where indicated, mice were injected with 0.2 ml of PBS only (control) or 0.2 ml of PBS containing flagellin. Flagellin treatment, unless indicated otherwise, used a dose of 20 µg and was given every other day from days 24-42 p.i. In parallel, the above mice were treated with PBS or PBS containing IL-22, IL-18, or both IL-22 and IL-18 as indicated.

Neutralization of IL-17 and IL-22. IL-17 and IL-22 were neutralized via i.p. injection of mAb to IL-17 (100 µg) and IL-22 (150 µg, clone 8E11) provided by Genentech, Inc. on days 0, 2, 4, 6 and 8 p.i. as previously described (*30, 31*)

ELISA to measure fecal RV antigens and antibodies. A sandwich enzyme-linked immunosorbent assay (ELISA) was performed to detect rotavirus antigen in mouse feces as previously described (*32*). Use of multiple dilutions of fecal suspension allowed determination of SD50. Serum anti-RV IgA or IgG and fecal anti-RV IgA were detected as previously described (*32*).

Immuonhistochemistry. Frozen mouse small intestinal sections were blocked with normal goat serum and incubated with a monoclonal antibody to rotavirus VP6 protein overnight at 4°C followed by 3 washes in PBS-Tween20. The slides were then incubated with biotinylated secondary antibody to mouse Ig diluted in PBS for 30 minutes at room temperature. After washing again, slides were incubated in HRP-Avidin in PBS for 30 minutes at room temperature. Then, 100 µl freshly made DAB substrate solution was applied to the slides to reveal color, followed by 3 washes in PBS-Tween20. Stained intestinal tissues were then dehydrated through 4 incubations in alcohol (95%, 95%, 100% and 100%). The color change provided by antibody staining was observed using microscopy.

Quantification of RV genomes and replication. Total RNA was isolated from tissues using TRIzol (Invitrogen, Carlsbad, CA), and quantitative RT-PCR (qRT-PCR) was performed using the Biorad iScript™ One-Step RT-PCR Kit in a CFX96 apparatus (Bio-Rad, Hercules, CA) with primers targeting the NSP3 region EC.C(+) (5-GTTCGTTGTGCCTCATTCG-3) and EC.C(-) (5-TCGGAACGTACTTCTGGAC-3). Strand-specific quantitative reverse transcription-PCR (ss-qRT-PCR) assay was used to quantify the ability of rotavirus to spread and replicate, as previously described (*33*).

Quantification of fecal reoviral RNA shedding using qRT-PCR. Reovirus T1L was generated as previously described (*34*). C57BL/6 mice were inoculated orally with 1-4 x 10^8 PFU of reovirus T1L in 0.2 ml PBS. From day 1 to 4 p.i., feces were collected, and total RNA was extracted according to the manufacturer's instructions (MO BIO, Inc., Carlsbad, CA). qRT-PCR was performed to determine viral shedding (forward primer 5′-CGCTTTTGAAGGTCGTGTATCA-3′ and reverse primer 5′-CTGGCTGTGCTGAGATTGTTTT-3′ corresponding to the viral S4 gene)(*35*). Viral shedding level was normalized to fecal weight (*36, 37*).

Quantification of host cell gene expression. Total RNA was isolated from colonic tissues using TRIzol (Invitrogen, Carlsbad, CA) according to the manufacturer's instructions, and qRT-PCR was performed using the Biorad iScript™ One-Step RT-PCR Kit in a CFX96 apparatus (Bio-Rad, Hercules, CA) with specific mouse oligonucleotides. The sense and antisense oligonucleotides used include the following: 36B4 5'-TCCAGGCTTTGGGCATCA-3' and 5'-CTTTATTCAGCTGCACATCACTCAGA-3'; KC 5'-TTGTGCGAAAAGAAGTGCAG-3' and 5'-TACAAACACAGCCTCCCACA-3'; IFN-λ 5'-AGCTGCAGGCCTTCAAAAAG-3' and 5'-TGGGAGTGAATGTGGCTCAG-3'; p40 5'-GACCATCACTGTCAAAGAGTTTCTAGAT-3' and
5'-AGGAAAGTCTTGTTTTTGAAATTTTTTAA-3'; IL-22 5'-GTGCTCAACTTCACCCTGGA-3' and 5'-TGGATGTTCTGGTCGTCACC-3'. Results were normalized to the housekeeping gene 36B4.

In vitro RV infection. HT-29 and Caco-2 cells were infected with cell culture-adapted rhesus rotavirus (EC strain cannot infect cultured cells) as previously described(*38*). 2x10^8 PFU of RRV was activated with 10 µg/ml of trypsin in serum free media (SFM) at 37°C for 30 minutes. HT-29

cells were grown to confluency in 6 well plates, washed several times with SFM, pre-treated with 100 ng/ml flagellin or left untreated (control). Two hours later, cells were inoculated with virus for 1 hour at 37°C/5% CO_2 to allow for adsorption (in the continued presence of flagellin). Following adsorption, cells were washed again several times with SFM and then incubated with 2 μg/ml trypsin in SFM for 0–48 hours p.i. For Caco-2 cells, Transwell plates (Corning Inc.) were used to allow cytokine treatment in the lower chamber and virus infection in the upper chamber. After IL-22/IL-18 pre-treatment for 1 hour, cells were infected in the presence of IL-22/IL-18 (maintained throughout experiment), and cell lysates prepared at indicated times.

Generation of bone marrow chimeric mice. Bone marrow chimeric mice were generated as previously described (*39*). Briefly, bone marrow cells were eluted from the femora and tibiae of donor mice with complete RPMI 1640 media. Recipient mice were irradiated at a dose of 11Gy with a ^{137}Cs irradiator before intravenous injection (i.v.) of $2x10^7$ donor bone marrow cells. After injection, the mice were maintained in sterile cages and supplied with drinking water containing 2 mg/ml of neomycin (Mediatech). Mice were utilized for experiments 8 weeks later. CD11c-DTR chimeras were used to deplete DC and avoid toxicity that results from DT administration to CD11c-DTR mice (*40*).

Cell depletion study. For depletion of NK cells, mice were treated with 200 μg of PK136 antibody to NK1.1 (Bio X Cell, Lebanon, NH) by i.p. injection every 2nd day from 2 days before infection to 8 days p.i. For neutrophil depletion, WT C57BL/6 mice were i.p. injected with 200 μg anti-Gr1 (RB6-8C5, Bio X Cell) every 2nd day from 2 days before RV infection to 8 days p.i. Chronically-infected *Rag1*$^{-/-}$ mice were injected with 500 μg anti-Gr1 every day from 3 days before flagellin treatment for 5 days. For depletion of macrophages, WT C57BL/6 mice were treated with 0.5 ml and 0.2 ml of clodronate liposomes (50 mg/ml) (ClodronateLiposome.org) by oral gavage and i.p., respectively, every 2nd day from 4 days before infection until day 0 p.i., after which time i.p. injection was continued to maintain depletion. For depletion of DCs, CD11c-DTR chimeric mice were treated with diphtheria toxin (DT, LIST Biological Laboratory, Inc.) at 8 ng/g body weight two and one days before RV infection.

Preparation of mouse whole blood leukocytes and lamina propria cells. Mouse blood was collected with heparinized tubes, centrifuged to removed plasma, resuspended in red blood lysis buffer (BD Biosciences) for 10 minutes, and washed in BD FACS buffer twice. Lamina propria cells were prepared as previously described (*41*).

Cell enrichment and adoptive transfer. WT C57BL/6 or *Tlr5*/*Nlrc4*$^{-/-}$ mice were injected with 30 μg Flt-3 ligand in 0.2 ml PBS every day for 9 days. Mouse splenocytes were stained with fluorochrome-conjugated antibodies to CD45, MHC class II, Ly6G, CD11c, CD11b, NK1.1, F4/80, CD3 and CD19. CD11c$^+$ DCs were FACS-sorted on a BD FACSAria III cell sorter. DC with about 99% purity were transferred to recipient mice by i.v. injection. Alternatively, mouse CD11c$^+$ DC were enriched by CD11c microbeads following the manufacturer's instruction (Miltenyi Biotec, Auburn, CA). The magnetically-enriched CD11c$^+$ DC with purity >95% were injected into *Tlr5*/*Nlrc4*$^{-/-}$ mice.

Flow cytometry analysis. Mouse whole blood leukocytes, splenocytes, and intestinal lamina propria cells were prepared and blocked with 10 μg/ml anti-CD16/anti-CD32 (clone 2.4G2 ATCC) for 10 minutes in FACS buffer (PBS supplemented with 0.5% BSA and 0.04% sodium azide). Aliquots of cells (1×10^6) were suspended in 0.1 ml FACS buffer on ice for 20 minutes with FITC-, PE-, PerCP-, APC-, PE-Cy7-, Alexa Fluor 700-, and Pacific blue-conjugated mAbs to detect the

following surface Ags: CD3, CD11b, CD11c, CD103, CD19, MHC class II, F4/80, NK1.1, CD45.1, CD45.2, Ly-6G (BD Biosciences). Stained cells were analyzed on a BD LSR II flow cytometer. Data analysis was carried out using FlowJo (TreeStar, Ashland, OR).

Isolation of Intestinal epithelial cells. Chronically RV-infected *Rag1*$^{-/-}$ mice were treated as indicated in the figures. At indicated times, mice were sacrificed and small intestines were washed extensively with PBS, cut to 1 cm pieces, and incubated with 2 mM EDTA for 30 minutes with shaking at 4^{o}C. After vortexing, the supernatant was passed through 100 μm cell strainer. The intestinal epithelial cells (IEC) were centrifuged, resuspended in PBS, and counted under a microscope.

SDS-PAGE Immunoblotting. At indicated time points following in vitro RV infection, cells were washed several times with cold PBS and resuspended in radioimmunoprecipitation assay II buffer (RIPA II) (20mM Tris-HCl, 2.5 mM EDTA, 1% Triton X-100, 10% glycerol, 1% deoxycholate, 0.1 % SDS, 50 mM NaF, 10 mM $Na_2P_2O_7$, 2 mM$NaV0_4$, and protease inhibitor cocktail). Cell lysates were separated on a precasted SDS-PAGE gel (Biorad), transferred to a nitrocellulose membrane, and probed with anti-rotavirus VP6 and human β-actin antibodies. To detect caspase 3, isolated IEC were incubated with 1X SDS lysis buffer (20mM Tris, pH6.8, 1% SDS, 1 mM EDTA) for 30 minutes at room temperature. After full-speed centrifugation, cell lysates were transferred to a fresh tube for analysis using antibodies to cleaved caspase 3 and β-actin antibodies (Cell Signaling Technology)

RNA sequencing. IEC were purified, as described above. RNA was extracted using Qiagen RNeasy kit, according to the manufacturer's protocol. After purification, RNA concentration and integrity were determined using Epoch Microplate Spectrophotometer (Bio-Tek) and agarose gel electrophoresis, respectively. Total RNA was then prepared for sequencing purposes, using Illumina TruSeq RNA kit, according to the manufacturer's protocol. Briefly, mRNA was purified using oligo-dT-coupled beads, fragmented, and converted to cDNA. After end repair and ligation of adapters, mRNA libraries were amplified by PCR and validated using BioAnalyser, according to manufacturer's recommendations. The purified library was then subjected to sequencing using a HiSeq machine at Cornell University's core facility. After quality filtering the data, adapter sequences were removed using fastqclipper tool (http://hannonlab.cshl.edu/fastx_toolkit/). Tophat2 (http://tophat.cbcb.umd.edu/) was then used to align sequences to the most recently updated *mus musculus* genome (mm10 version) based on the Bowtie algorithm (*42*). Alignment summary and normalization were performed through R using EdgeR package including tagwise negative binomial test (*43*). (http://www.bioconductor.org/packages/release/bioc/html/edgeR.html). The function plotSmear was used to generate plots of the log-fold-changes against log-cpm for each gene of the *mus musculus* genome. For pathway summarization, Panther classification system was used (*44*).

Figs. S1 to S21

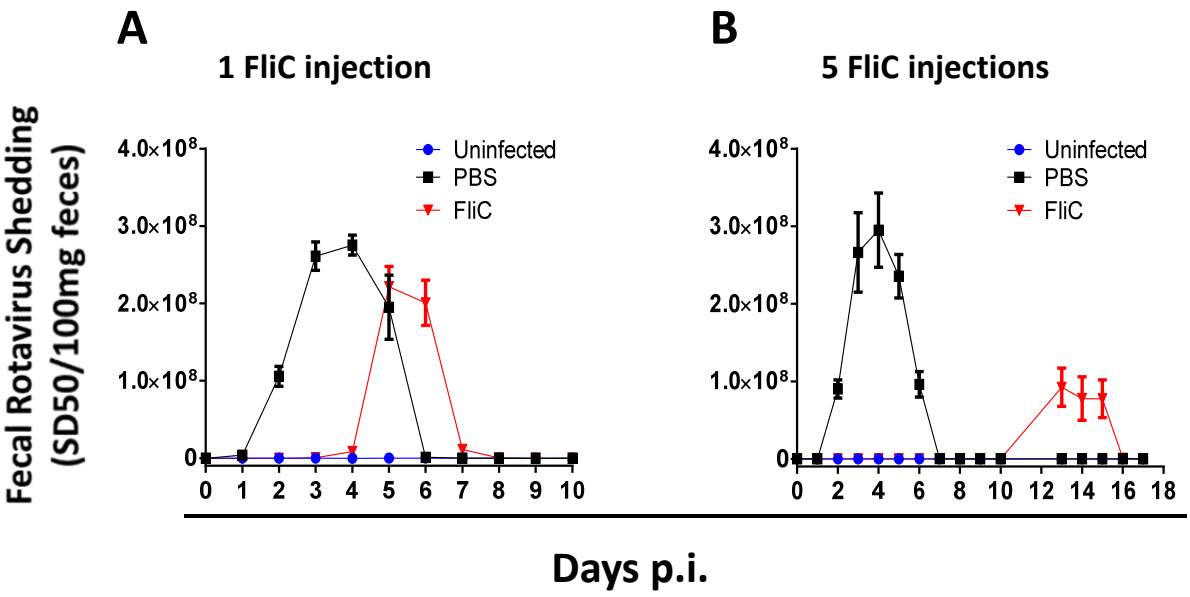

Fig. S1. Flagellin delays/protects mice from RV infection. (**A** and **B**) Eight-week-old female C57BL/6 mice were orally inoculated with murine RV, EC strain. Two hours prior to infection, mice were given an i.p. injection of 0.2 ml PBS (vehicle) or 0.2 ml of PBS containing 20 µg of flagellin. Feces were collected daily and assayed for RV antigens by ELISA. (A) Mice were administered PBS or flagellin only prior to inoculation with RV. (B) Mice were administered PBS or flagellin on day 0, 2, 4, 6 and 8 days p.i. Levels of fecal RV antigens shown as mean +/- S.E.M. The protection effect of flagellin versus PBS was statistically significant in (A) (Student's t-test, N=6, $P<0.0001$, on days 2-4) and (B) (2-way ANOVA, N=6, $P<0.001$).

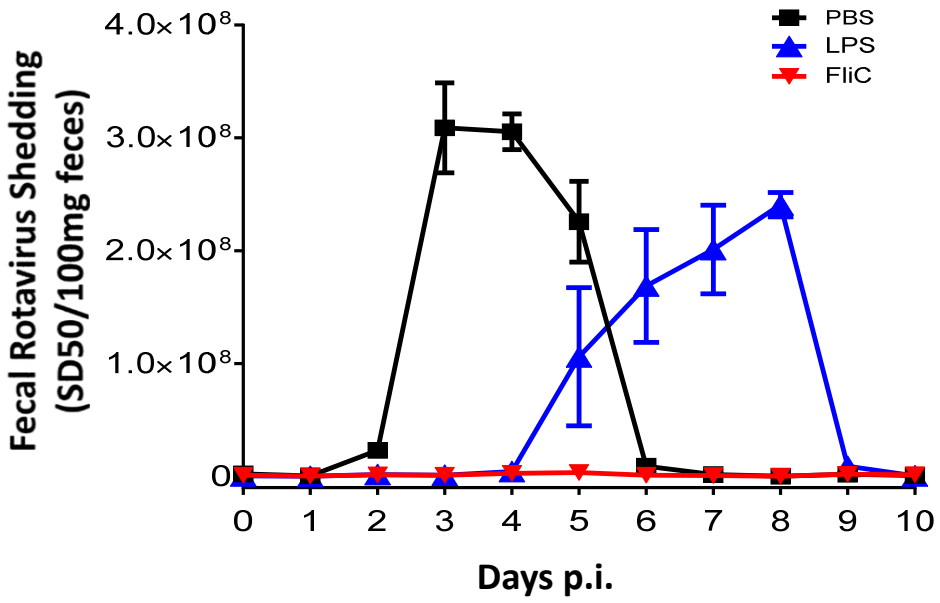

Fig. S2. LPS provides temporary protection against RV infection. Eight-week-old female C57BL/6 mice were orally inoculated with murine RV, EC strain. Mice were treated with PBS, LPS (10 μg), or flagellin (20 μg), via i.p. injection, every 2nd from day 0-8 p.i. Feces were collected daily and assayed for RV antigens by ELISA. Results are shown as mean +/- S.E.M. The difference was statistically significant between mice given PBS and flagellin (2-way ANOVA, N=5, $P<0.001$) and not significant between PBS and LPS (2-way ANOVA, N=5, $P=0.2147$).

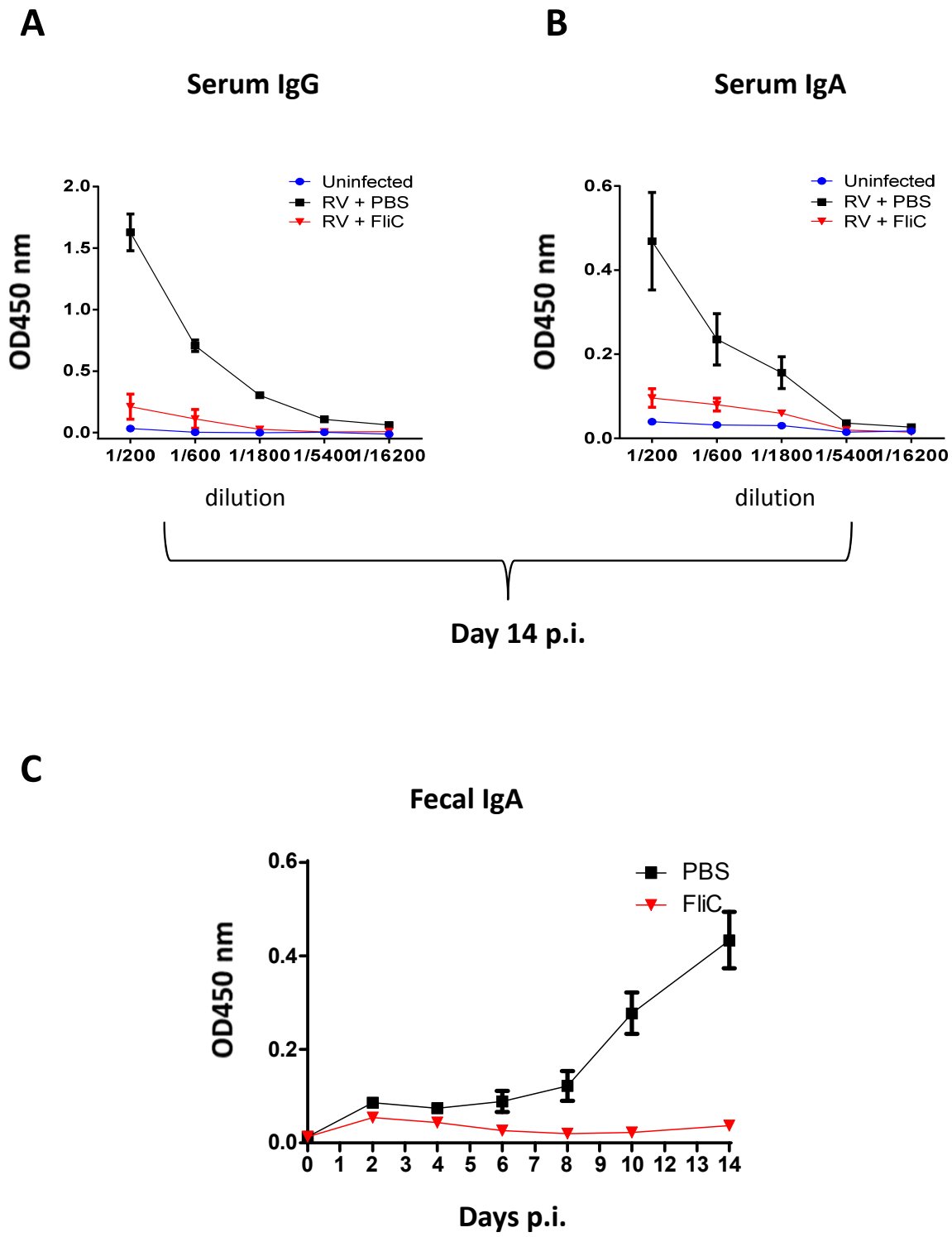

Fig. S3. Flagellin mediates prevention of RV infection without activating RV-specific adaptive immunity. (**A** to **C**) Sera and fecal samples from C57BL/6 mice, inoculated with RV and treated with PBS or flagellin as described in Fig. 1A, were isolated 14 days p.i. and assayed for anti-RV IgG (A) and IgA (B) by ELISA. Fecal samples on day 0, 2, 4, 6, 8, 10 and 14 p.i. were assayed for fecal IgA (C). The difference between mice given PBS and flagellin was statistically significantly from each other. Statistical analysis are shown as [Student's t-test, N=6, $P<0.001$, (A)], [Student's t-test, N=4, $P<0.05$, (B)] and [2-way ANOVA, N=5, $P<0.001$, (C)].

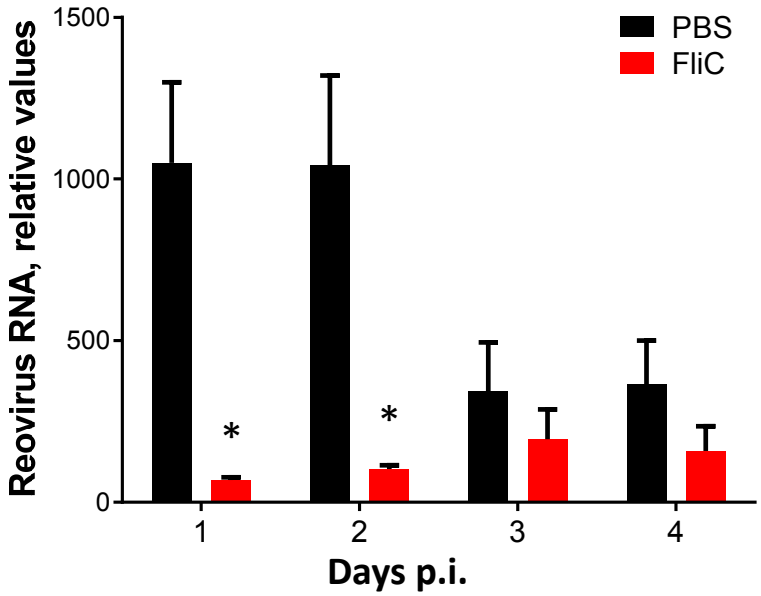

Fig. S4. Flagellin decreases fecal reovirus shedding in WT C57BL/6mice. C57BL/6 mice were inoculated per orally with 1-4 X 10^8 PFU of reovirus strain Type 1 Lang (T1L) in 0.2 ml PBS. Mice were i.p injected with PBS or flagellin (20 μg) 2 hours before reovirus inoculation and every second day thereafter. The number of viral genome copies in feces on days 1, 2, 3, and 4 was determined using qRT-PCR using primers specific to the reovirus S4 gene. Results are expressed as the mean +/- S.E.M. Asterisk indicates significant difference between untreated and flagellin-treated mice. (Student's t-test, N=4, *P<0.05).

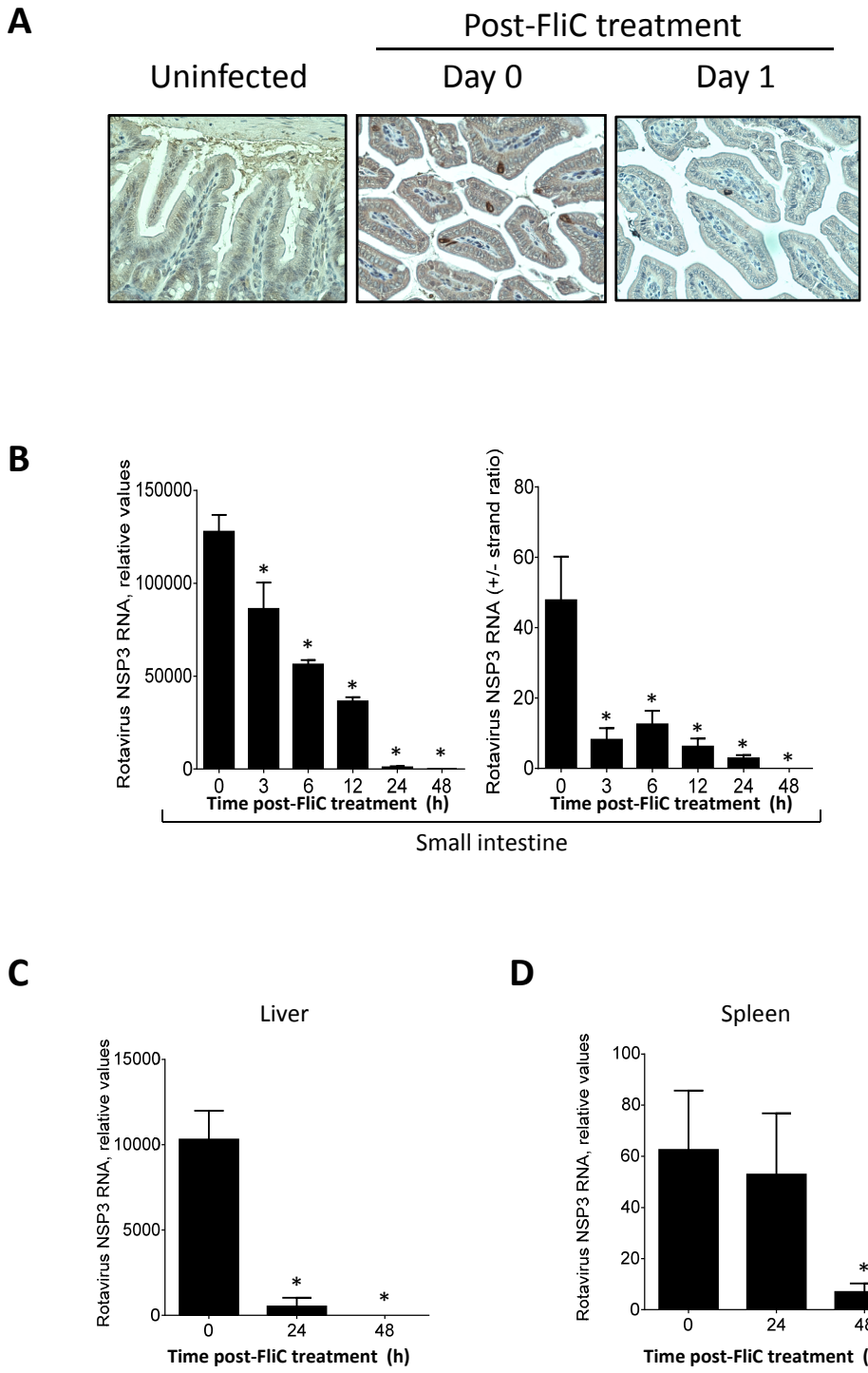

Fig. S5. Flagellin decreases RV antigen in chronically infected *Rag1*$^{-/-}$ mice. (**A**) Chronically RV-infected *Rag1*$^{-/-}$ mice were administered 1 dose of flagellin, euthanized day 1 after flagellin treatment and small intestine immunostained for RV antigens. Representative images are shown. (**B** to **D**) Chronically RV-infected *Rag1*$^{-/-}$ mice were administered 1 dose of flagellin, euthanized at 3, 6, 12, 24 and 48 hours. (B) Total RNA of small intestines were analyzed for NSP3 RNA level and ratio of positive strand to negative strand of NSP3 by strand-specific qRT-PCR which indicates viral replication rate). (C) Total RNA of liver were analyzed for RV NSP3 RNA level. (D) Total RNA of spleen were also analyzed for RV NSP3 RNA level. Asterisk indicates significant difference between untreated and flagellin-treated mice. [Student t-test, N=3, *P<0.05, for (B), (C) and (D)].

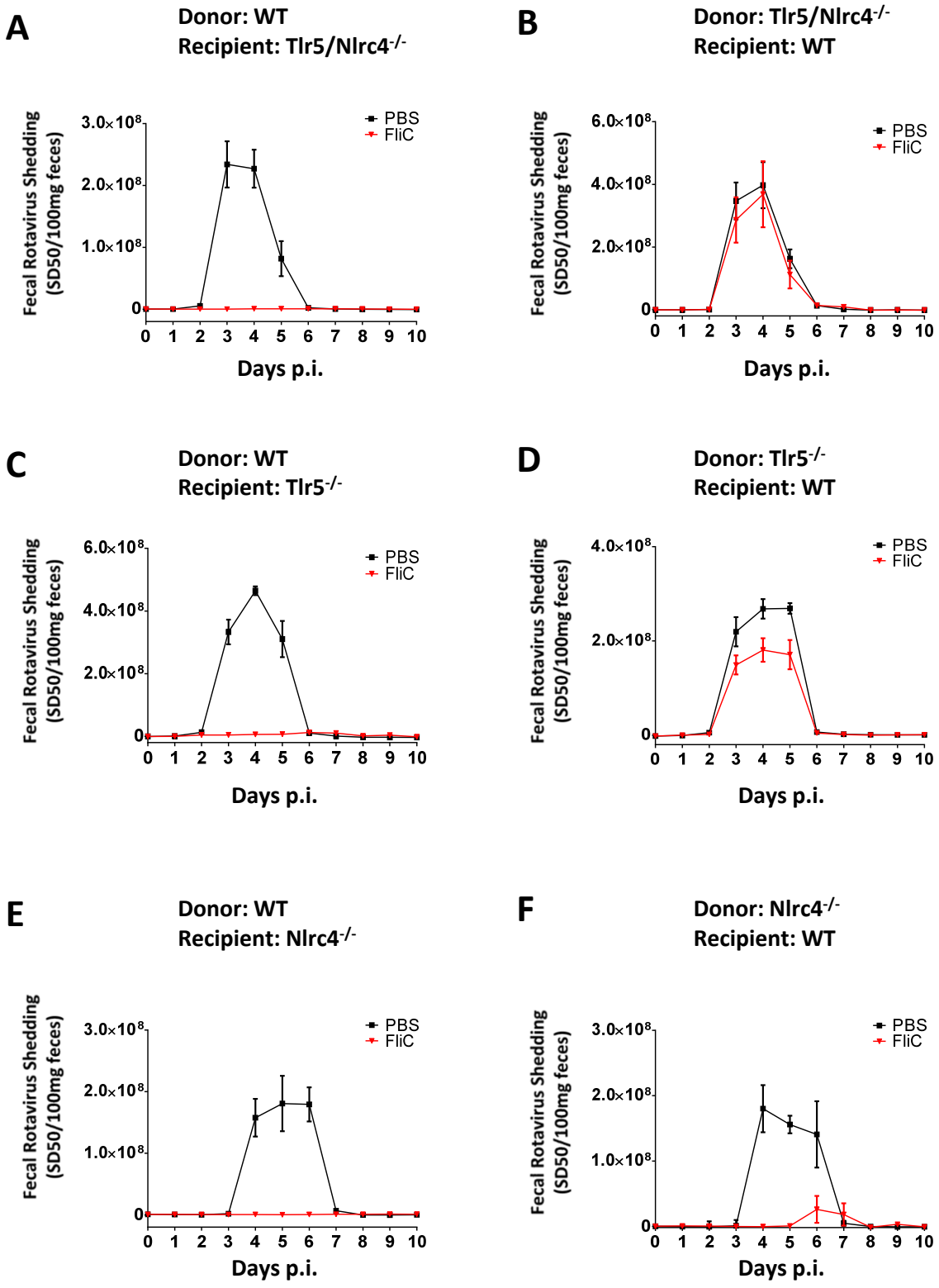

Fig. S6. Flagellin's antiviral activity requires TLR5 on hematopoietic cells and NLRC4 in either compartment. (**A** to **F**) Indicated bone marrow chimeric mice were inoculated with RV and treated with PBS or flagellin from day 0-8 p.i. Feces were collected daily and assayed for RV antigens by ELISA. Measure of RV antigens in feces, are shown as mean +/- S.E.M. The difference between mice given PBS and flagellin was statistically significant in (A) (2-way ANOVA, N=6-7, $P<0.001$) and [(C) to (F)] (2-way ANOVA, N=4-8, $P<0.001$), and non-significant in (B) (2-way ANOVA, N=5, $P=0.4183$).

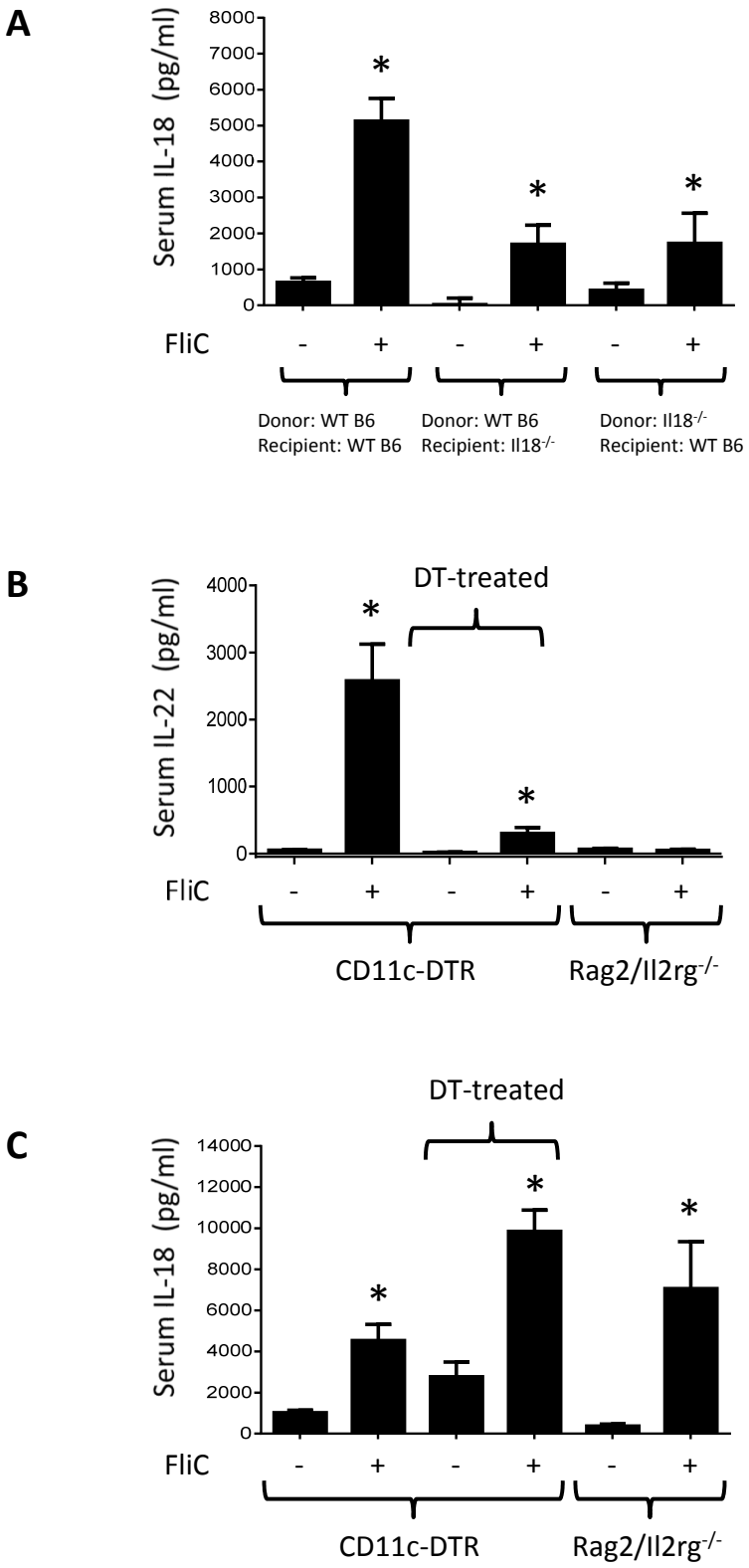

Fig. S7. Cellular source of flagellin-induced IL-18 and IL-22. (**A**) Bone marrow chimeric mice generated from WT and *Il18*$^{-/-}$ mice were treated with flagellin. Sera were collected at 3 hours post treatment and assayed for IL-18 by ELISA (Student's t-test, N=4-5, *P<0.01). (**B** and **C**) CD11c-DTR mice were injected with DT. After 24 hours, the CD11c-DTR and *Rag2/Il2rg*$^{-/-}$ mice were treated with flagellin, and, 3 hours post flagellin treatment, sera were assayed for IL-22 (B) and IL-18 (C) by ELISA (Student's t-test, N=3-4, *P<0.05). Asterisk indicates significant difference between untreated and flagellin-treated mice.

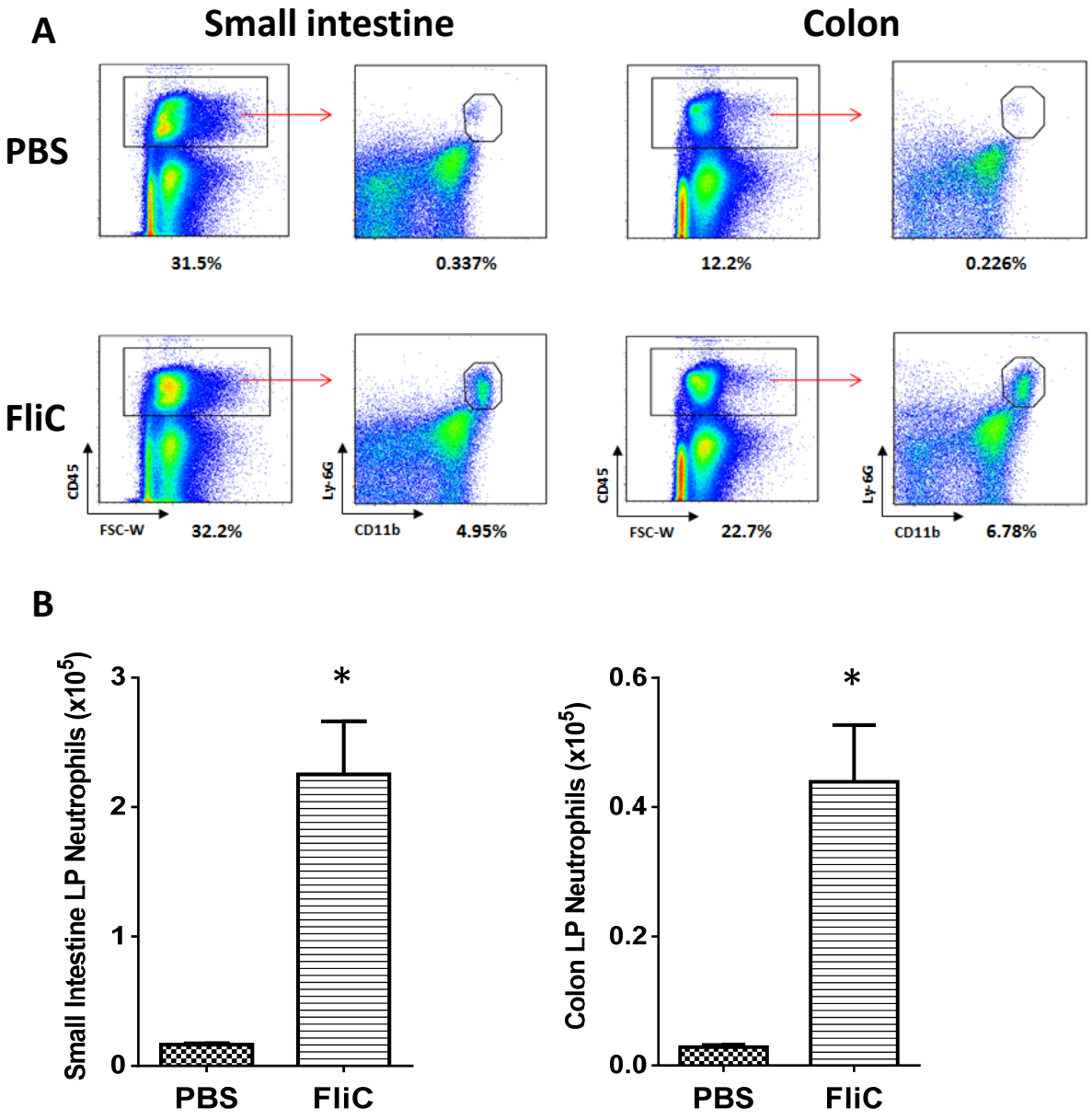

Fig. S8. Flagellin-treated RV-infected mice exhibit massive neutrophil infiltration in the gut. (**A** and **B**) *Rag1*$^{-/-}$ mice were orally inoculated with murine RV, EC strain. Mice were treated with PBS or flagellin (20 μg), via i.p. injection, in day 0 and 2 p.i. On day 3 p.i., lamina propria of small intestines and colons were analyzed for neutrophil infiltration by flow cytometry. (A) Scatter plots using CD45, Ly-6G, and CD11b to quantitate relative numbers of neutrophils in each condition/tissue. (B) Mean quantitation of neutrophils +/- S.E.M. Induction of small intestinal and colonic neutrophils by flagellin was significant (Student's t-test, N=4, *P<0.01) for both tissues.

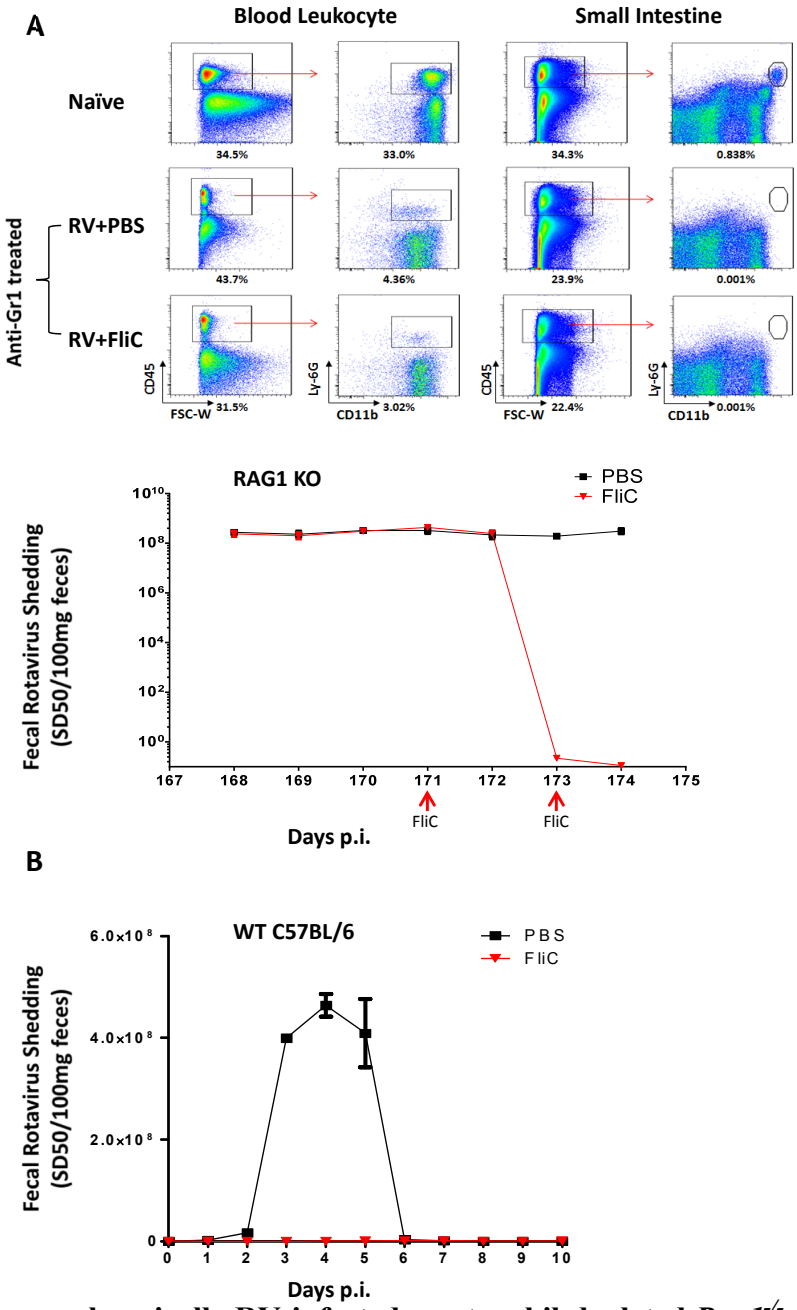

Fig. S9. Flagellin cures chronically RV-infected, neutrophil-depleted *Rag1*$^{-/-}$ mice and prevents RV infection in neutrophil-depleted WT C57BL/6 mice. (**A** and **B**) (A) *Rag1*$^{-/-}$ mice, which had been chronically infected with RV for 168 days were subjected to antibody-mediated neutrophil depletion beginning day 168 p.i. and then treated with PBS or 20 μg flagellin on day 171 and 173 p.i. Feces were collected on indicated day and assayed for RV antigens by ELISA. Mice were euthanized on day 174 at which time intestinal tissue was assayed for relative numbers of neutrophils as in Fig. S8. Relative numbers of neutrophils in each condition/tissue and levels of fecal RV antigens shown as mean +/- S.E.M were shown. Differences between PBS and flagellin groups were significant (2-way ANOVA, N=3, P<0.01) beginning 2 days post-treatment. (B) Eight-week-old C57BL/6 mice were treated with neutrophil-depleting antibody 24 hours before RV infection and then once every 2nd day from day 0-8 p.i. The mice were given PBS or 20 μg flagellin 2 hours before RV inoculation. Feces were assayed for RV antigens by ELISA. Differences between PBS and flagellin groups were significant (2-way ANOVA, N=4, P<0.0001).

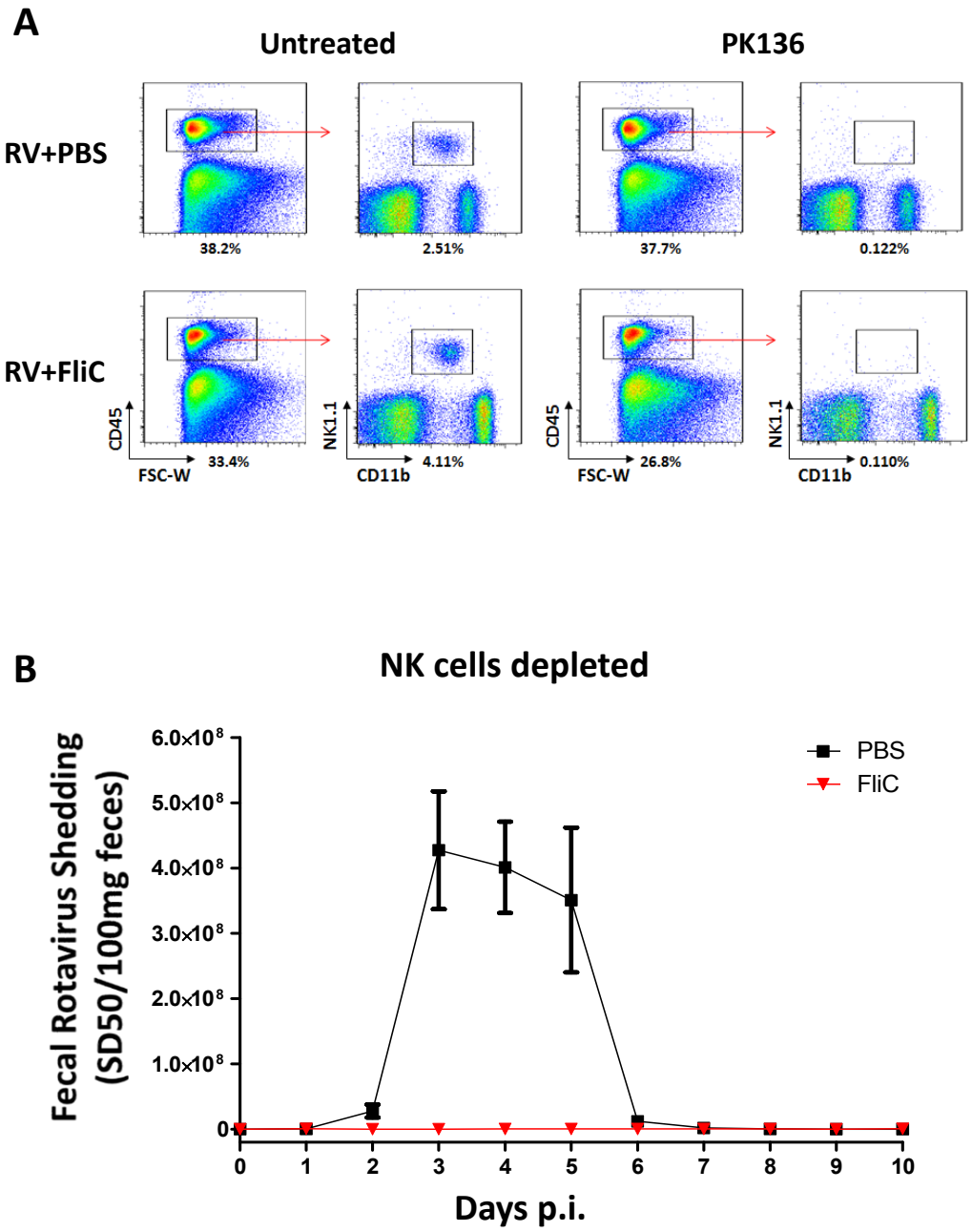

Fig. S10. Flagellin-induced antiviral effect is maintained in mice depleted of NK cells. (**A** and **B**) C57BL/6 mice were subjected to antibody-mediated NK cell depletion. Two days later, mice were orally inoculated with RV and treated via i.p. injection with PBS or flagellin (20 μg) every 2nd day from day 0-8 p.i. Feces were collected daily and assayed for RV antigens by ELISA. (A) Scatter plots using CD45, NK1.1 and CD11b to quantitate relative numbers of NK cells in each condition. (B) Levels of fecal RV antigens shown as mean +/- S.E.M. The difference between mice given PBS and flagellin was statistically significant (2-way ANOVA, N=4, $P<0.001$).

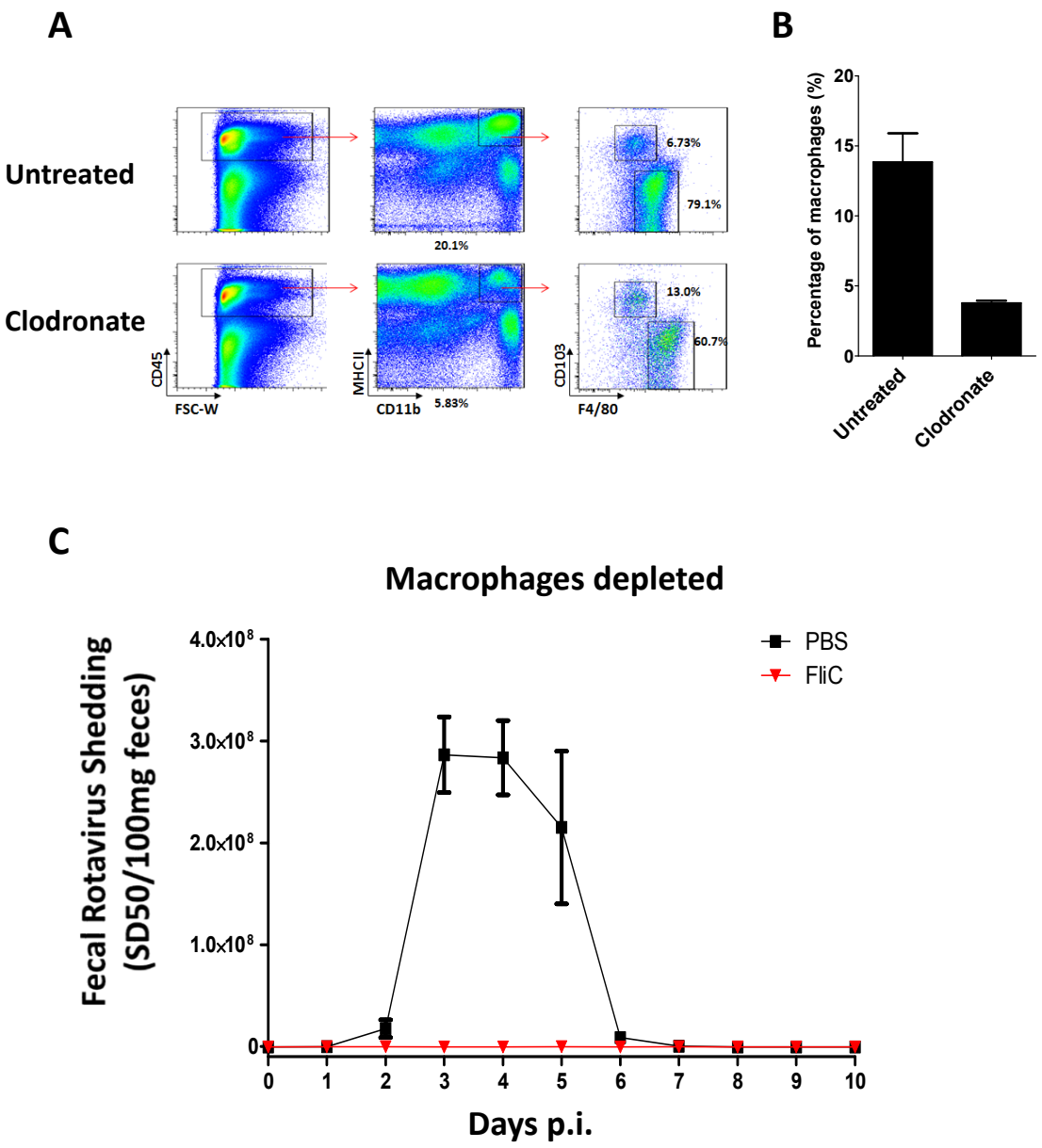

Fig. S11. Flagellin-induced antiviral effects are maintained in mice depleted of macrophages. (**A** to **C**) C57BL/6 mice were subjected to clodronate liposome-mediated macrophage depletion from 4 days before infection. Clodronate liposome-treated mice were orally inoculated with RV and treated via i.p. injection with PBS or flagellin (20 μg) every 2nd day from day 0-8 p.i. Feces were collected daily and assayed for RV antigens by ELISA. (A) Scatter plots using CD45, MHC class II, CD11b and F4/80 to quantitate relative numbers of macrophages in each condition and (B) percentage of decrease of macrophages after depletion was calculated. (C) Levels of fecal RV antigens shown as mean +/- S.E.M. The difference between mice given PBS and flagellin was statistically significant (2-way ANOVA, N=4, $P<0.001$).

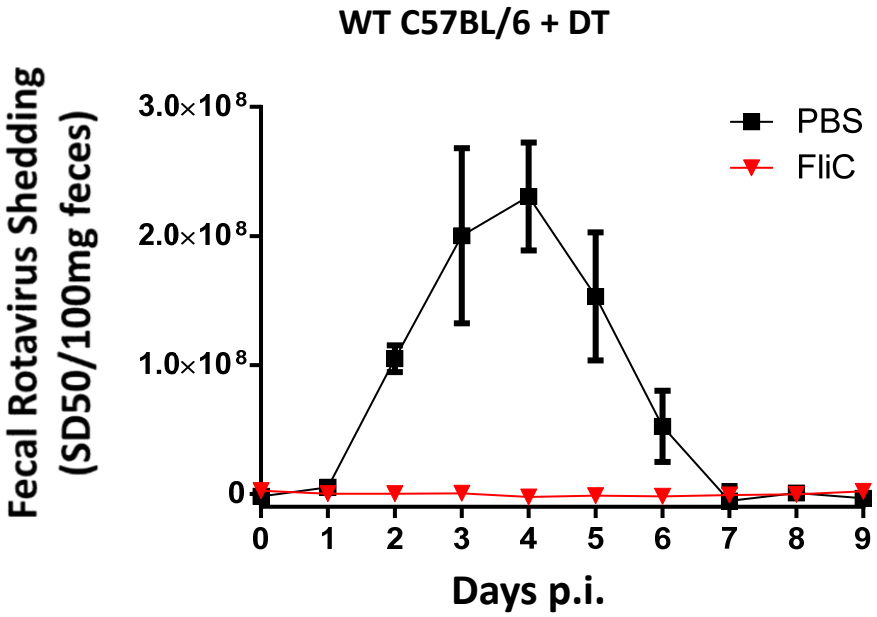

Fig. S12. Diphtheria toxin does not affect flagellin-mediated protection against RV in WT C57BL/6 mice from RV. (**A** and **B**) Eight-week-old female C57BL/6 mice were treated DT on 2 consecutive days. Twenty-four hours after the second DT treatment, the mice were orally inoculated with murine RV, EC strain. Two hours prior to infection and every 2nd day thereafter from day 0-8 p.i., mice were given an i.p. injection of 0.2 ml PBS (vehicle) or 0.2 ml of PBS containing 20 µg of flagellin. Feces were collected daily and assayed for RV antigens by ELISA. Levels of fecal RV antigens shown as mean +/- S.E.M. The difference between flagellin and PBS was statistically significant (2-way ANOVA, N=5, $P<0.001$).

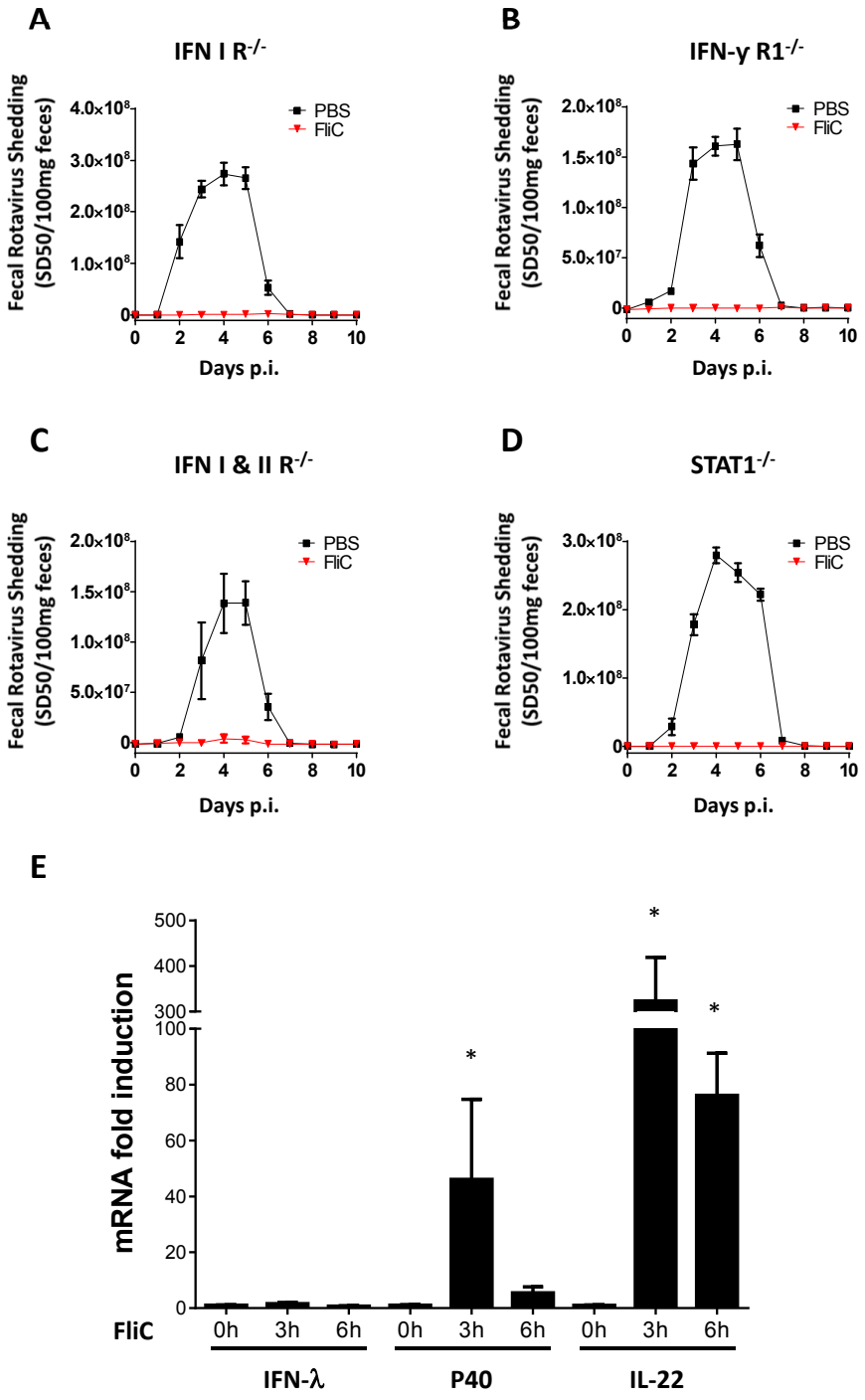

Fig. S13. Flagellin induces intestinal expression of IL-12/IL-23 and IL-22 but not type III IFN. (**A to D**) Indicated strains of genetically-modified 8-week-old mice were orally inoculated with murine RV, EC strain. Mice were treated with PBS or flagellin (20 μg), via injection, every other day from 0-8 days p.i. Feces were collected daily and assayed for RV antigens by ELISA. (A) IFN I $R^{-/-}$, (B) IFNγ$R1^{-/-}$, (C) IFN I & II $R^{-/-}$, (D) $STAT1^{-/-}$. Levels of fecal RV antigens shown as mean +/- S.E.M. The difference between mice given PBS and flagellin was statistically significant for (A) to (D) (2-way ANOVA, N=5-6, P<0.0001). (**E**) *Rag1*$^{-/-}$ mice were administered 20 μg of flagellin and euthanized at indicated time point. Small intestinal mRNA level of indicated genes was measured by qRT-PCR. Data are shown as means +/- S.E.M. Asterisk indicates significant difference between untreated and flagellin-treated mice (Student's t-test, N=3-6, *P<0.05).

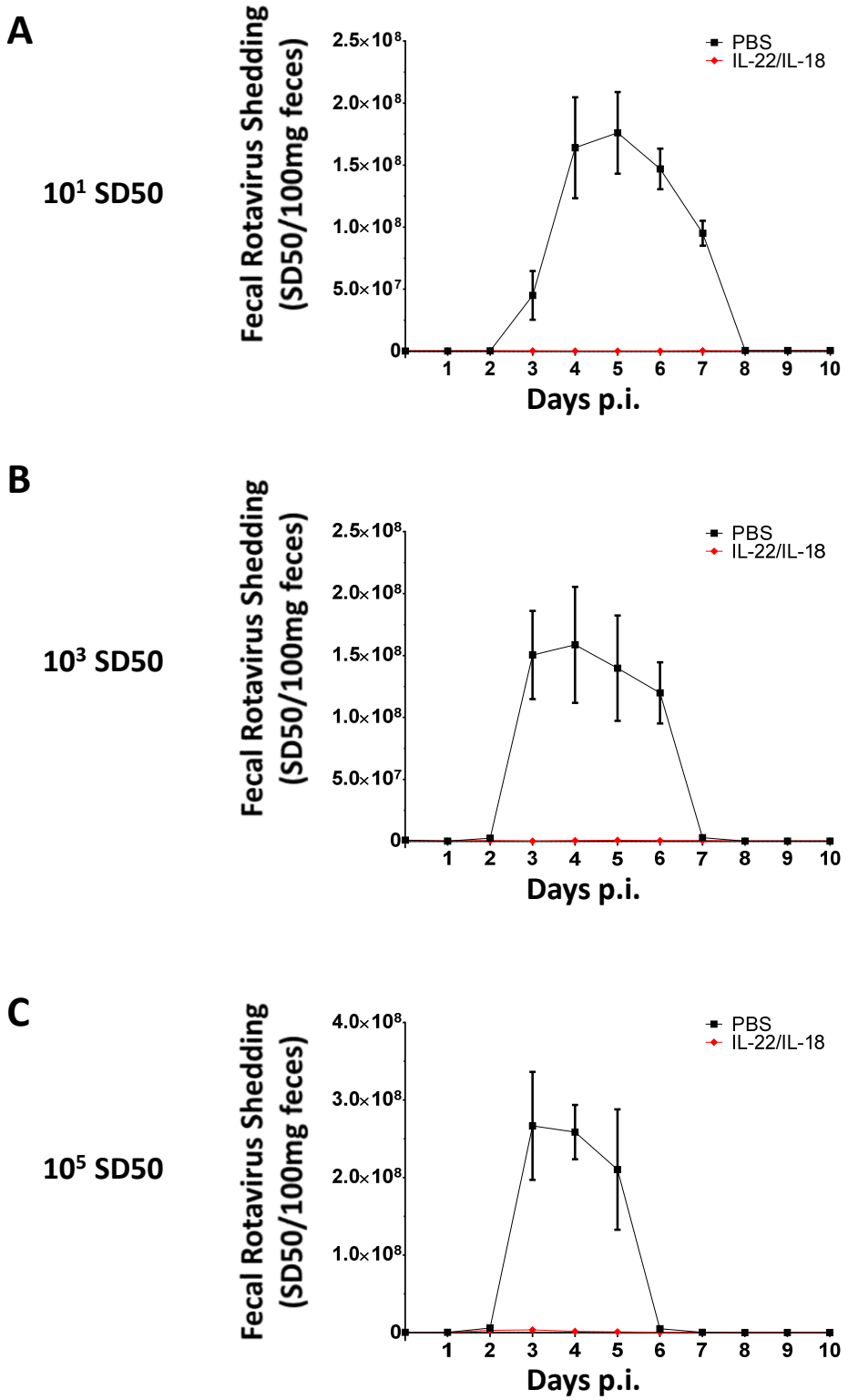

Fig. S14. IL-22/IL-18 protects WT C57BL/6 mice against high and low levels of RV inocula. (**A** to **C**) Eight-week-old female C57BL/6 mice were orally inoculated with (A) 10^1, (B) 10^3 and (C) 10^5 SD50 of murine RV. Two hours prior to infection and every 2nd day thereafter from day 0-8 p.i., mice were given an i.p. injection of 0.2 ml PBS (vehicle) or 0.2 ml of PBS containing 2 μg of IL-22 and 1 μg of IL-18. Feces were collected daily and assayed for RV antigens by ELISA. Levels of fecal RV antigens shown as mean +/- S.E.M. The protection effect of IL-22/IL-18 versus PBS was statistically significant in all three groups (2-way ANOVA, N=5, $P<0.001$).

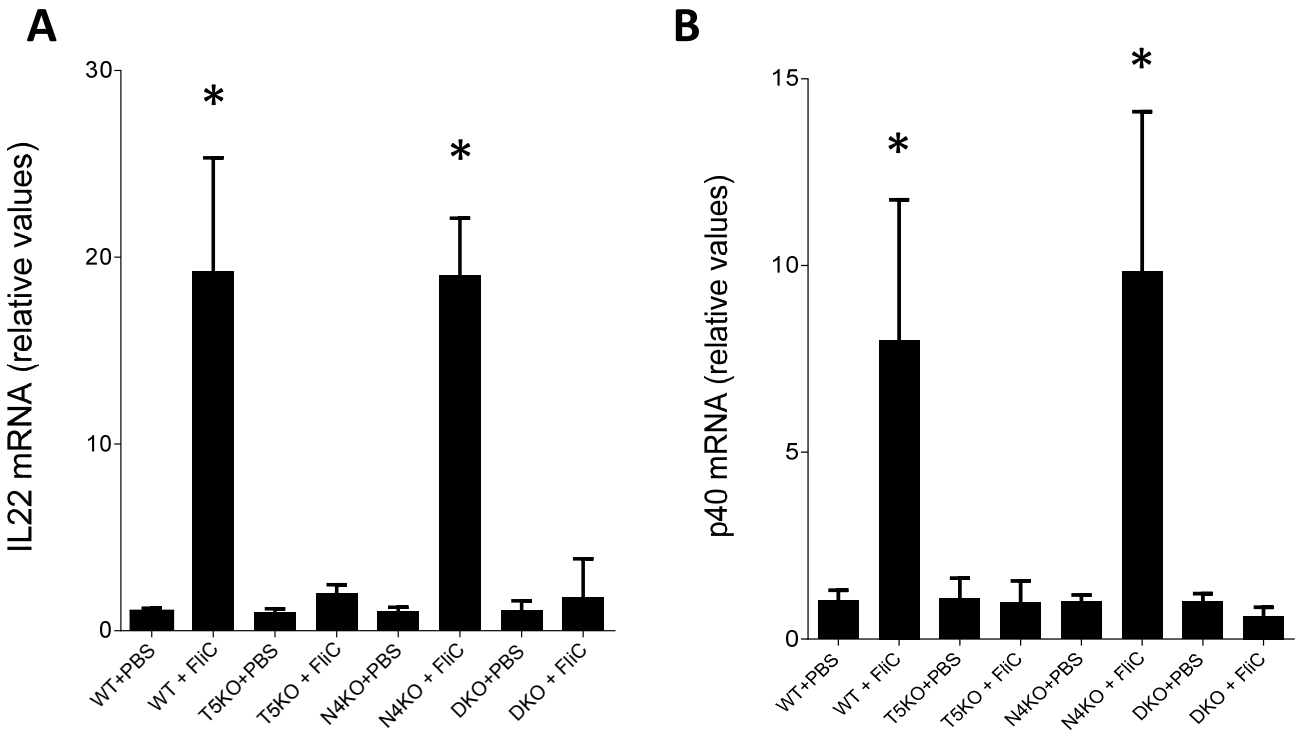

Fig. S15. Flagellin-induced activation of IL-22 is independent of NLRC4 signaling. (**A** and **B**) WT C57BL/6, TLR5$^{-/-}$, NLRC4$^{-/-}$, and TLR5/NLRC4$^{-/-}$ mice were administered 20 μg of flagellin and euthanized at 3 hours. Small intestinal mRNA level of IL-22 (A) and p40 (B) was measured by qRT-PCR. Data are the means +/- S.E.M. Asterisk indicates significant difference between PBS and flagellin-treated mice (Student's t-test, N=4, *P<0.05).

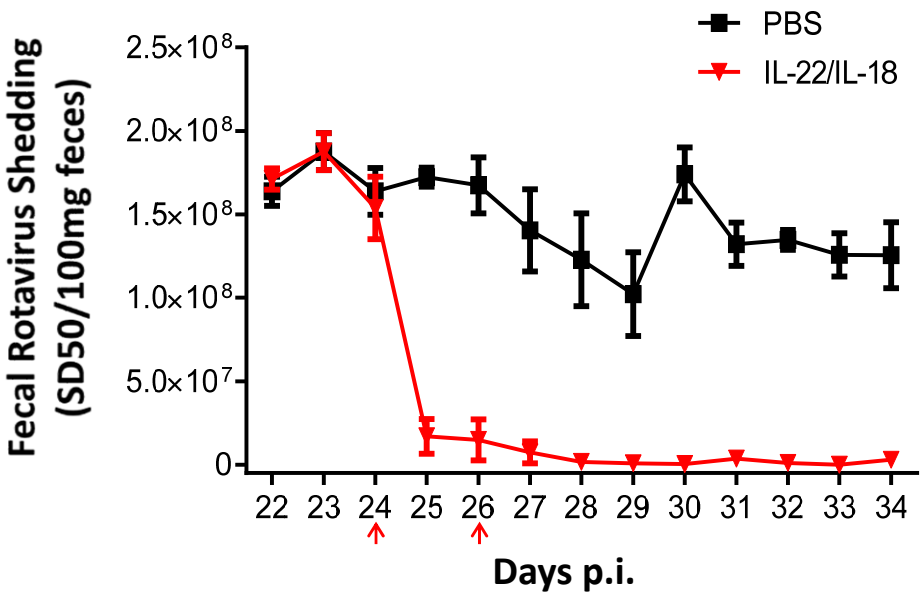

Fig. S16. IL-22/IL-18 treatment cures chronically RV-infected *Rag2/Il2rg*$^{-/-}$ mice. Three-week-old *Rag2/Il2rg*$^{-/-}$ mice were inoculated with murine RV. Three weeks following inoculation, mice were treated with PBS, 10 μg IL-22 plus 1 μg IL-18 by i.p. injection on day 24 and 26 p.i. as indicated by red arrows. Feces were collected daily until day 34 p.i. and assayed for RV antigens by ELISA. Results are shown as the mean +/- S.E.M (2-way ANOVA, N=3, $P<0.0001$).

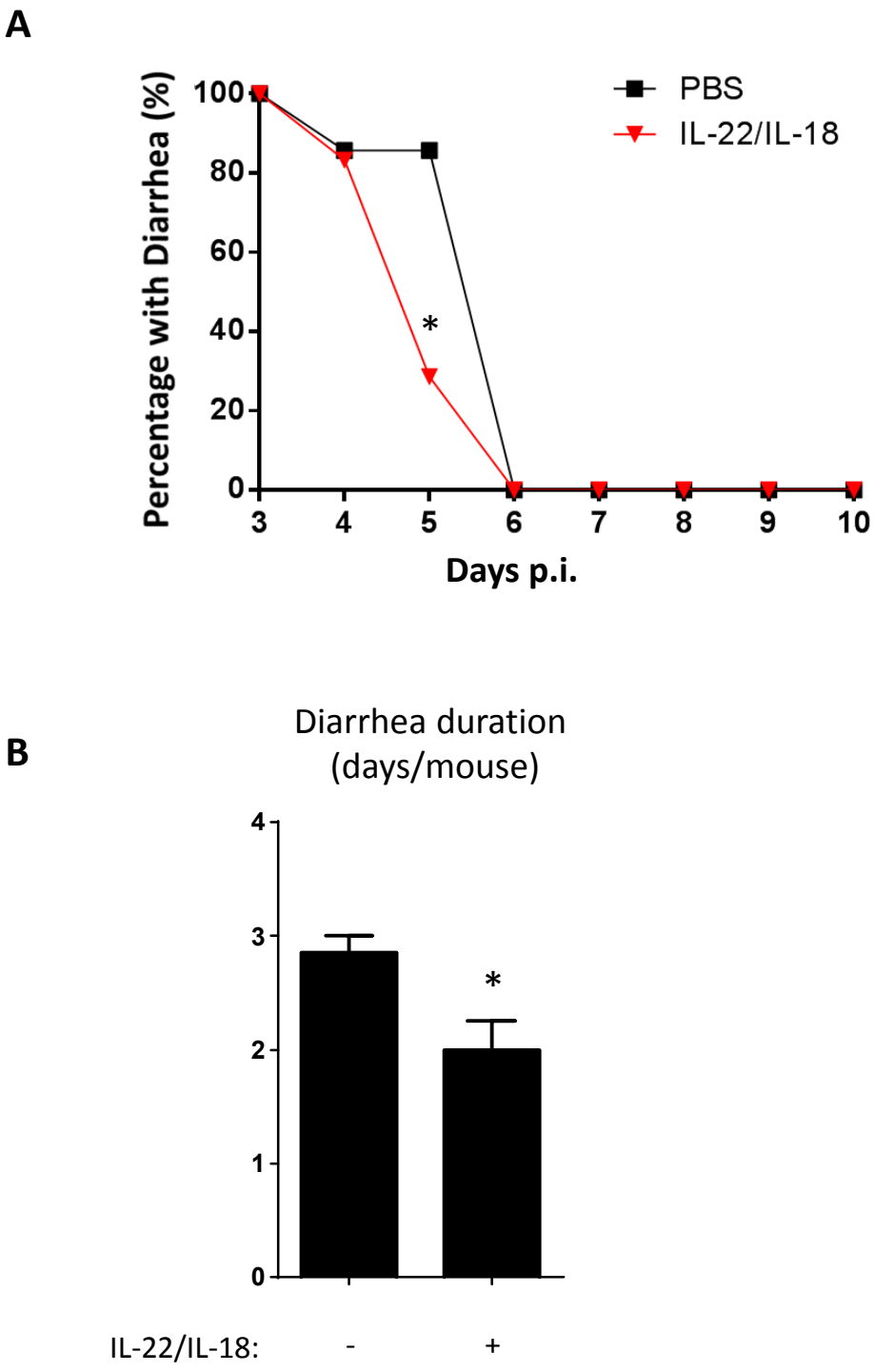

Fig. S17. IL-22/IL-18 treatment shortens duration of established diarrhea in young C57BL/6 mice. (**A** and **B**) Seven-day old C57BL/6 mice were orally inoculated with RV as described in Methods. Three days after inoculation, at which time 100% of mice exhibited diarrhea, mice were treated with 50 μl PBS (vehicle) or 50 μl PBS containing 2 μg IL-22 plus 0.2 μg IL-18 by i.p. injection every day from 3-9 days p.i. and monitored for (A) incidence of diarrhea daily (Chi-square test, N=6,7, * $P<0.01$) and (B) duration of diarrhea after IL-22/IL-18 treatment (Student t-test, N=6, 7, *$P<0.05$). Asterisk indicates significant difference between untreated and flagellin-treated mice.

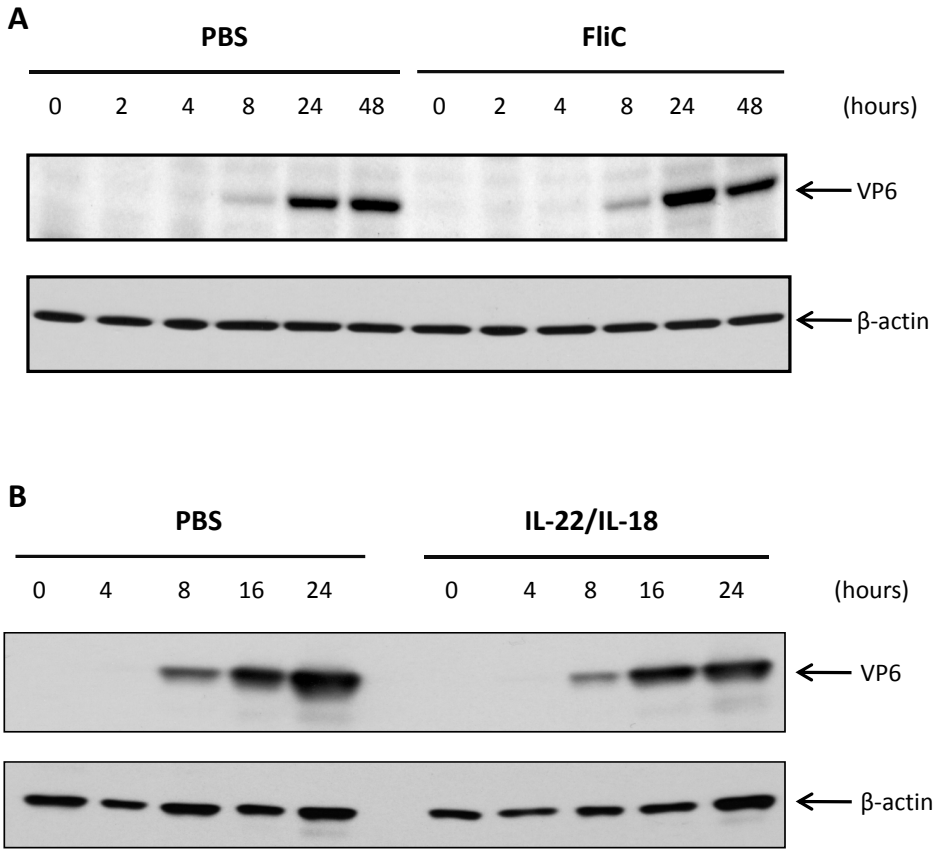

Fig. S18. Flagellin and IL-22/IL-18 treatment does not affect RV infection/replication significantly in cultured intestinal epithelial cells. (**A**) Confluent monolayers of intestinal epithelial (HT-29) cells were pretreated with flagellin (100 ng/ml) 2 hours before infecting with rhesus RV at multiplicity of infection of 1.0. At indicated time points, cell lysates were analyzed for the RV antigen VP6, as an indicator of infection/replication, by SDS-PAGE immunoblotting. Data is representative of 5 experiments, which showed similar lack of effect of flagellin on RV infection/replication in vitro. (**B**) Polarized monolayers of Caco-2 cells, cultured on collagen-coated permeable supports, were basolaterally treated with recombinant human IL-22/IL-18 (100 ng/ml of each cytokine) 1 hour before infection with Rhesus RV at multiplicity of infection of 1.0. At indicated time points cell lysates were analyzed for the RV antigen VP6, as an indicator of infection/replication, by SDS-PAGE immunoblotting. Results are from a single experiment and representative of 3 experiments that showed similar results.

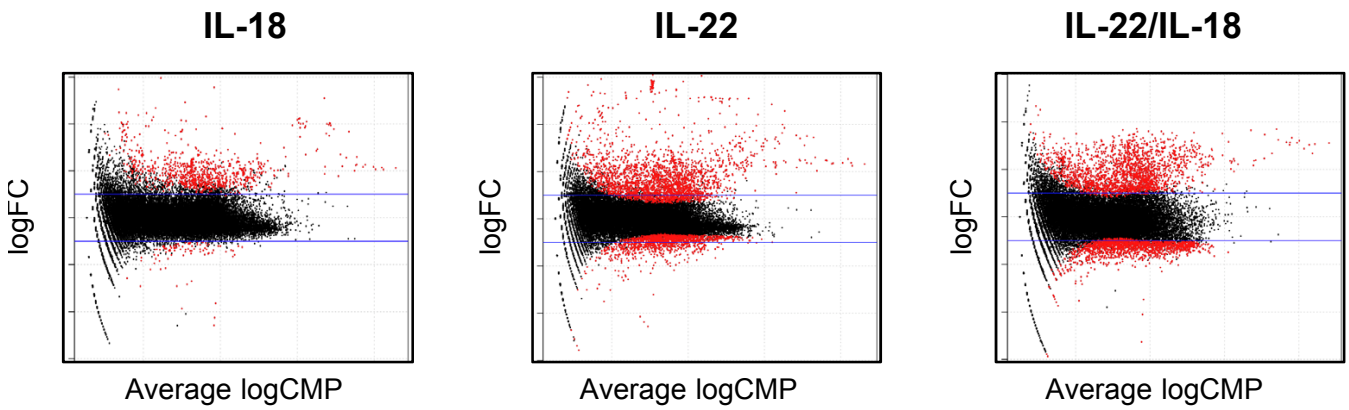

Fig. S19. Major remodeling of IEC gene expression in vivo by IL-22 but not IL-18. RNA sequencing data were generated as described in Methods, and the function plotSmear of EdgeR package for R was used to generate plots of the log-fold-changes against log-cpm, for each gene of the *mus musculus* genome (mm10). Genes with significantly modified expression in the treated group compared to the control group were plotted in red, using exact test function of EdgeR which is conducting tagwise tests using the exact negative binomial test. The horizontal blue lines showed 2-fold changes (N= 3, significance determined as described in Methods).

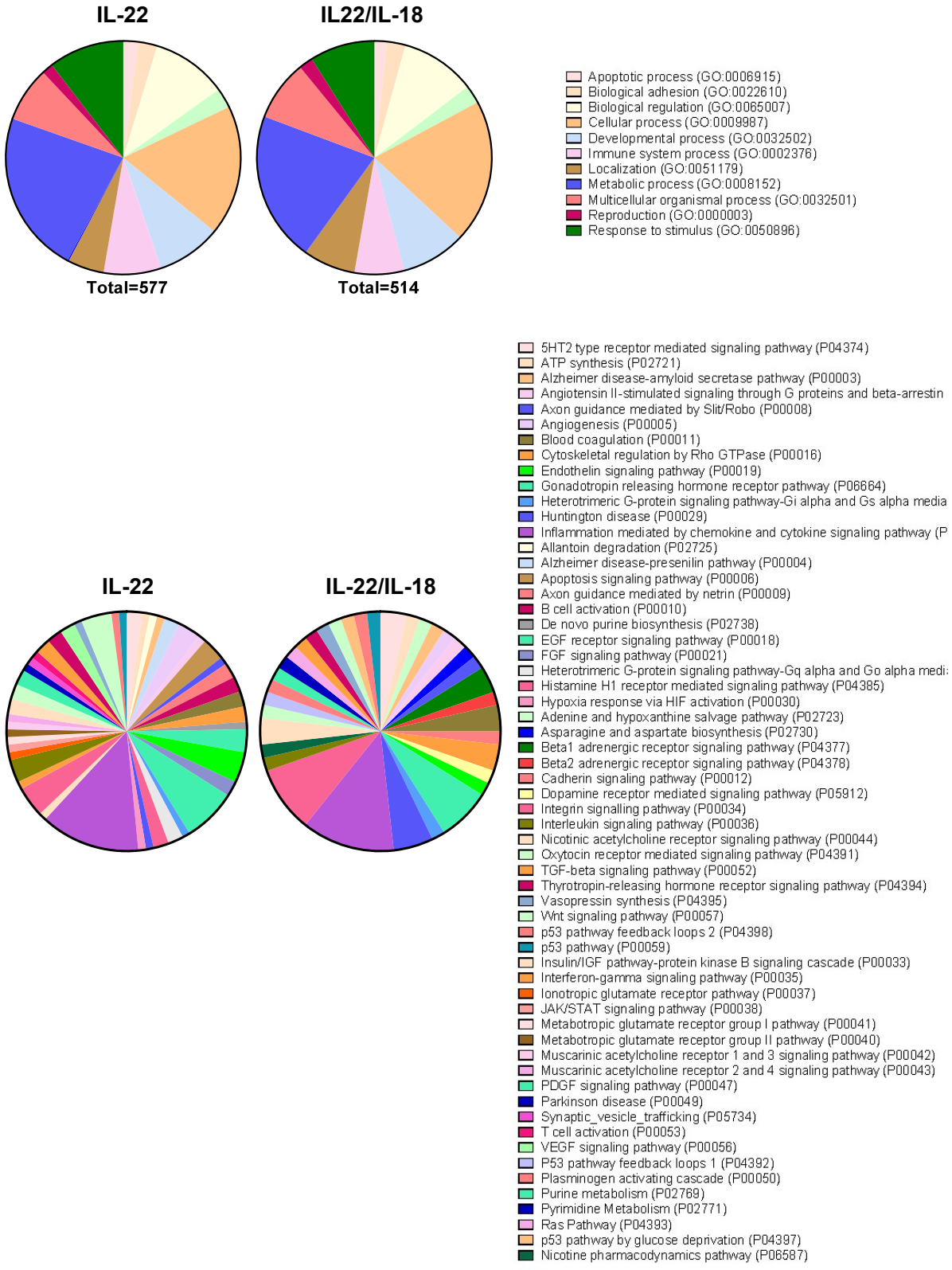

Fig. S20. Processes and pathways altered in IL-22 and IL-22/IL-18 treated mice.
RNA sequencing data were generated as described in the full method. Genes with significantly increased expression in treated group compare to control group were determined using exact test function of EdgeR. The list of Ensembl gene IDs obtained was then summarized in biological process (upper panel) and pathway (lower panel) using Panther Classification System. (N= 3, significance determined as described in Methods).

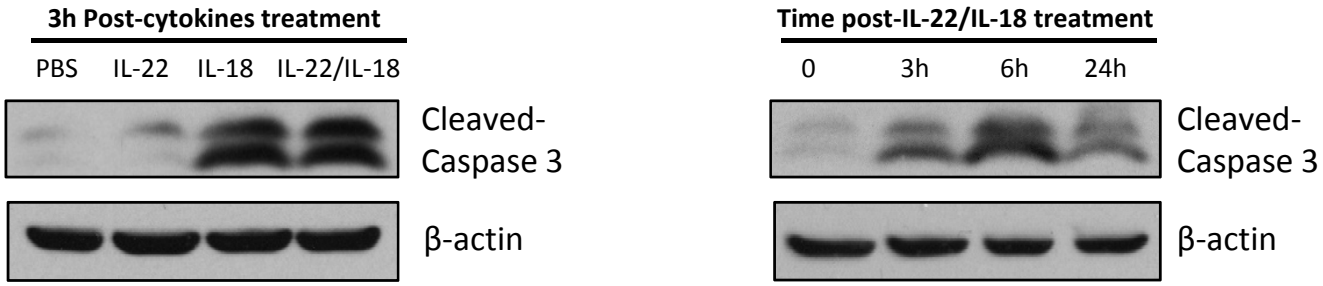

Fig. S21. IL-22 and IL-22/IL-18 treatment induces cell death in RV-infected IEC. Chronically RV-infected *Rag1*$^{-/-}$ mice were treated with 1 injection of PBS, PBS containing 10 μg IL-22, 1 μg IL-18 or 10 μg IL-22 plus 1 μg IL-18. At indicated time, the mice were sacrificed and intestinal epithelial cells IEC were prepared from small intestines. Whole cell lysates from above IEC were analyzed by SDS-PAGE immunoblotting with antibodies to cleaved caspase 3. **Left panel** shows results of 3 hours after different cytokines treatment and **right panel** shows results of indicated time points of IL-22/IL-18 treatment. Results are from a single experiment and representative of 3 experiments that showed similar results.

References and Notes

1. H. B. Greenberg, M. K. Estes, Rotaviruses: From pathogenesis to vaccination. *Gastroenterology* **136**, 1939–1951 (2009). Medline doi:10.1053/j.gastro.2009.02.076

2. N. Feng, M. A. Franco, H. B. Greenberg, Murine model of rotavirus infection. *Adv. Exp. Med. Biol.* **412**, 233–240 (1997). Medline doi:10.1007/978-1-4899-1828-4_35

3. H. Zeng, A. Q. Carlson, Y. Guo, Y. Yu, L. S. Collier-Hyams, J. L. Madara, A. T. Gewirtz, A. S. Neish, Flagellin is the major proinflammatory determinant of enteropathogenic Salmonella. *J. Immunol.* **171**, 3668–3674 (2003). Medline doi:10.4049/jimmunol.171.7.3668

4. M. Vijay-Kumar, A. T. Gewirtz, Flagellin: Key target of mucosal innate immunity. *Mucosal Immunol.* **2**, 197–205 (2009). Medline doi:10.1038/mi.2009.9

5. R. M. Jones, V. M. Sloane, H. Wu, L. Luo, A. Kumar, M. V. Kumar, A. T. Gewirtz, A. S. Neish, Flagellin administration protects gut mucosal tissue from irradiation-induced apoptosis via MKP-7 activity. *Gut* **60**, 648–657 (2011). Medline doi:10.1136/gut.2010.223891

6. L. G. Burdelya, V. I. Krivokrysenko, T. C. Tallant, E. Strom, A. S. Gleiberman, D. Gupta, O. V. Kurnasov, F. L. Fort, A. L. Osterman, J. A. Didonato, E. Feinstein, A. V. Gudkov, An agonist of toll-like receptor 5 has radioprotective activity in mouse and primate models. *Science* **320**, 226–230 (2008). Medline doi:10.1126/science.1154986

7. M. Vijay-Kumar, J. D. Aitken, C. J. Sanders, A. Frias, V. M. Sloane, J. Xu, A. S. Neish, M. Rojas, A. T. Gewirtz, Flagellin treatment protects against chemicals, bacteria, viruses, and radiation. *J. Immunol.* **180**, 8280–8285 (2008). Medline doi:10.4049/jimmunol.180.12.8280

8. A. Sen, N. Feng, K. Ettayebi, M. E. Hardy, H. B. Greenberg, IRF3 inhibition by rotavirus NSP1 is host cell and virus strain dependent but independent of NSP1 proteasomal degradation. *J. Virol.* **83**, 10322–10335 (2009). Medline doi:10.1128/JVI.01186-09

9. J. Q. Jiang, X. S. He, N. Feng, H. B. Greenberg, Qualitative and quantitative characteristics of rotavirus-specific CD8 T cells vary depending on the route of infection. *J. Virol.* **82**, 6812–6819 (2008). Medline doi:10.1128/JVI.00450-08

10. J. M. Ball, P. Tian, C. Q. Zeng, A. P. Morris, M. K. Estes, Age-dependent diarrhea induced by a rotaviral nonstructural glycoprotein. *Science* **272**, 101–104 (1996). Medline doi:10.1126/science.272.5258.101

11. I. Uhnoo, M. Riepenhoff-Talty, T. Dharakul, P. Chegas, J. E. Fisher, H. B. Greenberg, P. L. Ogra, Extramucosal spread and development of hepatitis in immunodeficient and normal mice infected with rhesus rotavirus. *J. Virol.* **64**, 361–368 (1990). Medline

12. F. A. Carvalho, I. Nalbantoglu, J. D. Aitken, R. Uchiyama, Y. Su, G. H. Doho, M. Vijay-Kumar, A. T. Gewirtz, Cytosolic flagellin receptor NLRC4 protects mice against mucosal and systemic challenges. *Mucosal Immunol.* **5**, 288–298 (2012). Medline doi:10.1038/mi.2012.8

13. A. Kupz, G. Guarda, T. Gebhardt, L. E. Sander, K. R. Short, D. A. Diavatopoulos, O. L. Wijburg, H. Cao, J. C. Waithman, W. Chen, D. Fernandez-Ruiz, P. G. Whitney, W. R. Heath, R. Curtiss 3rd, J. Tschopp, R. A. Strugnell, S. Bedoui, NLRC4 inflammasomes in dendritic cells regulate noncognate effector function by memory $CD8^+$ T cells. *Nat. Immunol.* **13**, 162–169 (2012). Medline doi:10.1038/ni.2195

14. M. Vijay-Kumar, F. A. Carvalho, J. D. Aitken, N. H. Fifadara, A. T. Gewirtz, TLR5 or NLRC4 is necessary and sufficient for promotion of humoral immunity by flagellin. *Eur. J. Immunol.* **40**, 3528–3534 (2010). Medline doi:10.1002/eji.201040421

15. L. Franchi, A. Amer, M. Body-Malapel, T. D. Kanneganti, N. Ozören, R. Jagirdar, N. Inohara, P. Vandenabeele, J. Bertin, A. Coyle, E. P. Grant, G. Núñez, Cytosolic flagellin requires Ipaf for activation of caspase-1 and interleukin 1β in salmonella-infected macrophages. *Nat. Immunol.* **7**, 576–582 (2006). Medline doi:10.1038/ni1346

16. S. Nordlander, J. Pott, K. J. Maloy, NLRC4 expression in intestinal epithelial cells mediates protection against an enteric pathogen. *Mucosal Immunol.* **7**, 775–785 (2014). Medline

17. M. A. Kinnebrew, C. G. Buffie, G. E. Diehl, L. A. Zenewicz, I. Leiner, T. M. Hohl, R. A. Flavell, D. R. Littman, E. G. Pamer, Interleukin 23 production by intestinal $CD103^+CD11b^+$ dendritic cells in response to bacterial flagellin enhances mucosal innate immune defense. *Immunity* **36**, 276–287 (2012). Medline doi:10.1016/j.immuni.2011.12.011

18. S. Jung, D. Unutmaz, P. Wong, G. Sano, K. De los Santos, T. Sparwasser, S. Wu, S. Vuthoori, K. Ko, F. Zavala, E. G. Pamer, D. R. Littman, R. A. Lang, In vivo depletion of $CD11c^+$ dendritic cells abrogates priming of $CD8^+$ T cells by exogenous cell-associated antigens. *Immunity* **17**, 211–220 (2002). Medline doi:10.1016/S1074-7613(02)00365-5

19. J. Pott, T. Mahlakõiv, M. Mordstein, C. U. Duerr, T. Michiels, S. Stockinger, P. Staeheli, M. W. Hornef, IFN-λ determines the intestinal epithelial antiviral host defense. *Proc. Natl. Acad. Sci. U.S.A.* **108**, 7944–7949 (2011). Medline doi:10.1073/pnas.1100552108

20. M. Vijay-Kumar, J. R. Gentsch, W. J. Kaiser, N. Borregaard, M. K. Offermann, A. S. Neish, A. T. Gewirtz, Protein kinase R mediates intestinal epithelial gene remodeling in response to double-stranded RNA and live rotavirus. *J. Immunol.* **174**, 6322–6331 (2005). Medline doi:10.4049/jimmunol.174.10.6322

21. L. Van Maele, C. Carnoy, D. Cayet, P. Songhet, L. Dumoutier, I. Ferrero, L. Janot, F. Erard, J. Bertout, H. Leger, F. Sebbane, A. Benecke, J. C. Renauld, W. D. Hardt, B. Ryffel, J. C. Sirard, TLR5 signaling stimulates the innate production of IL-17 and IL-22 by $CD3^-$ $CD127^+$ immune cells in spleen and mucosa. *J. Immunol.* **185**, 1177–1185 (2010). Medline

22. B. Chassaing, R. E. Ley, A. T. Gewirtz, Intestinal epithelial cell Toll-like receptor 5 regulates the intestinal microbiota to prevent low-grade inflammation and metabolic syndrome in mice. *Gastroenterology* 10.1053/j.gastro.2014.08.033 (2014). Medline doi:10.1053/j.gastro.2014.08.033

23. U. D. Parashar, C. J. Gibson, J. S. Bresee, R. I. Glass, Rotavirus and severe childhood diarrhea. *Emerg. Infect. Dis.* **12**, 304–306 (2006). Medline doi:10.3201/eid1202.050006

24. J. W. Graff, K. Ettayebi, M. E. Hardy, Rotavirus NSP1 inhibits NFkappaB activation by inducing proteasome-dependent degradation of β-TrCP: A novel mechanism of IFN antagonism. *PLOS Pathog.* **5**, e1000280 (2009). Medline doi:10.1371/journal.ppat.1000280

25. Y. Zhao, J. Yang, J. Shi, Y. N. Gong, Q. Lu, H. Xu, L. Liu, F. Shao, The NLRC4 inflammasome receptors for bacterial flagellin and type III secretion apparatus. *Nature* **477**, 596–600 (2011). Medline doi:10.1038/nature10510

26. A. T. Gewirtz, T. A. Navas, S. Lyons, P. J. Godowski, J. L. Madara, Cutting edge: Bacterial flagellin activates basolaterally expressed TLR5 to induce epithelial proinflammatory gene expression. *J. Immunol.* **167**, 1882–1885 (2001). Medline doi:10.4049/jimmunol.167.4.1882

27. A. T. Gewirtz, P. O. Simon Jr., C. K. Schmitt, L. J. Taylor, C. H. Hagedorn, A. D. O'Brien, A. S. Neish, J. L. Madara, *Salmonella typhimurium* translocates flagellin across intestinal epithelia, inducing a proinflammatory response. *J. Clin. Invest.* **107**, 99–109 (2001). Medline doi:10.1172/JCI10501

28. S. J. McSorley, B. D. Ehst, Y. Yu, A. T. Gewirtz, Bacterial flagellin is an effective adjuvant for $CD4^+$ T cells in vivo. *J. Immunol.* **169**, 3914–3919 (2002). Medline doi:10.4049/jimmunol.169.7.3914

29. C. J. Sanders, L. Franchi, F. Yarovinsky, S. Uematsu, S. Akira, G. Núñez, A. T. Gewirtz, Induction of adaptive immunity by flagellin does not require robust activation of innate immunity. *Eur. J. Immunol.* **39**, 359–371 (2009). Medline doi:10.1002/eji.200838804

30. R. Basu, D. B. O'Quinn, D. J. Silberger, T. R. Schoeb, L. Fouser, W. Ouyang, R. D. Hatton, C. T. Weaver, Th22 cells are an important source of IL-22 for host protection against enteropathogenic bacteria. *Immunity* **37**, 1061–1075 (2012). Medline doi:10.1016/j.immuni.2012.08.024

31. J. M. Kezic, T. T. Glant, J. T. Rosenbaum, H. L. Rosenzweig, Neutralization of IL-17 ameliorates uveitis but damages photoreceptors in a murine model of spondyloarthritis. *Arthritis Res. Ther.* **14**, R18 (2012). Medline doi:10.1186/ar3697

32. R. Uchiyama, B. Chassaing, B. Zhang, A. T. Gewirtz, Antibiotic treatment suppresses rotavirus infection and enhances specific humoral immunity. *J. Infect. Dis.* **210**, 171–182 (2014). Medline doi:10.1093/infdis/jiu037

33. M. Fenaux, M. A. Cuadras, N. Feng, M. Jaimes, H. B. Greenberg, Extraintestinal spread and replication of a homologous EC rotavirus strain and a heterologous rhesus rotavirus in BALB/c mice. *J. Virol.* **80**, 5219–5232 (2006). Medline doi:10.1128/JVI.02664-05

34. A. Berard, K. M. Coombs, Mammalian reoviruses: Propagation, quantification, and storage. *Curr. Protoc. Microbiol.* **chap. 15**, Unit15C 1 (2009).

35. K. W. Boehme, J. M. Frierson, J. L. Konopka, T. Kobayashi, T. S. Dermody, The reovirus sigma1s protein is a determinant of hematogenous but not neural virus dissemination in mice. *J. Virol.* **85**, 11781–11790 (2011). Medline doi:10.1128/JVI.02289-10

36. C. Johansson, J. D. Wetzel, J. He, C. Mikacenic, T. S. Dermody, B. L. Kelsall, Type I interferons produced by hematopoietic cells protect mice against lethal infection by

mammalian reovirus. *J. Exp. Med.* **204**, 1349–1358 (2007). Medline doi:10.1084/jem.20061587

37. L. S. Ooms, T. Kobayashi, T. S. Dermody, J. D. Chappell, A post-entry step in the mammalian orthoreovirus replication cycle is a determinant of cell tropism. *J. Biol. Chem.* **285**, 41604–41613 (2010). Medline doi:10.1074/jbc.M110.176255

38. A. H. Frias, M. Vijay-Kumar, J. R. Gentsch, S. E. Crawford, F. A. Carvalho, M. K. Estes, A. T. Gewirtz, Intestinal epithelia activate anti-viral signaling via intracellular sensing of rotavirus structural components. *Mucosal Immunol.* **3**, 622–632 (2010). Medline doi:10.1038/mi.2010.39

39. C. J. Sanders, D. A. Moore 3rd, I. R. Williams, A. T. Gewirtz, Both radioresistant and hemopoietic cells promote innate and adaptive immune responses to flagellin. *J. Immunol.* **180**, 7184–7192 (2008). Medline doi:10.4049/jimmunol.180.11.7184

40. T. Zaft, A. Sapoznikov, R. Krauthgamer, D. R. Littman, S. Jung, CD11chigh dendritic cell ablation impairs lymphopenia-driven proliferation of naive and memory $CD8^+$ T cells. *J. Immunol.* **175**, 6428–6435 (2005). Medline doi:10.4049/jimmunol.175.10.6428

41. T. L. Denning, Y. C. Wang, S. R. Patel, I. R. Williams, B. Pulendran, Lamina propria macrophages and dendritic cells differentially induce regulatory and interleukin 17-producing T cell responses. *Nat. Immunol.* **8**, 1086–1094 (2007). Medline doi:10.1038/ni1511

42. B. Langmead, C. Trapnell, M. Pop, S. L. Salzberg, Ultrafast and memory-efficient alignment of short DNA sequences to the human genome. *Genome Biol.* **10**, R25 (2009). Medline doi:10.1186/gb-2009-10-3-r25

43. M. D. Robinson, G. K. Smyth, Small-sample estimation of negative binomial dispersion, with applications to SAGE data. *Biostatistics* **9**, 321–332 (2008). Medline doi:10.1093/biostatistics/kxm030

44. H. Mi, A. Muruganujan, J. T. Casagrande, P. D. Thomas, Large-scale gene function analysis with the PANTHER classification system. *Nat. Protoc.* **8**, 1551–1566 (2013). Medline doi:10.1038/nprot.2013.092

45. Throughout **the** manuscript, ~~*N*~~ ***n*** refers to **the** number of mice per experimental condition.